Output-feedback stabilization in prescribed-time of a class of reaction-diffusion PDEs with boundary input delay

Salim Zekraoui, Nicolás Espitia, Wilfrid Perruquetti, Miroslav Krstic

Output-feedback stabilization in prescribed-time of a class of reaction-diffusion PDEs with boundary input delay

Salim Zekraoui[1], Nicolas Espitia[2], Wilfrid Perruquetti[3], and Miroslav Krstic[4]

***Abstract*— Time-varying prescribed-time (PT) controllers use growing gains not only to achieve convergence in desired time but to reduce state peaking during stabilization and to also reduce the control effort by distributing it more evenly over the time interval of convergence. In this paper, we consider a one-dimensional reaction-diffusion system with boundary input delay and propose a general method for studying the problem of prescribed-time boundary stabilization. To achieve this objective, we first reformulate the system as a PDE-PDE cascade system (i.e., a cascade of a linear transport partial differential equation (PDE) with a linear reaction-diffusion PDE), where the transport equation represents the effect of the input delay. We then apply a time-varying infinite-dimensional backstepping transformation to convert the cascade system into a prescribed-time stable (in short PTS) target system. The stability analysis is conducted on the target system, and the desired stability property is transferred back to the closed-loop system using the inverse transformation. The effectiveness of the proposed approach is demonstrated through numerical simulations.**

***Index Terms*— Prescribed-time stability, finite-time stability, delay systems, reaction-diffusion equation, transport equation, input delay, cascade PDE-PDE system, backstepping approach**

I. Introduction

A. Literature on stabilization of reaction-diffusion PDEs with input delay:

In processes modeled by reaction-diffusion systems (biological, chemical, epidemiological, etc), feedback action may be considerably delayed. These delays, in particular delays of the inputs, have to be taken into account in the control design as they may induce instabilities in the closed-loop system. The stabilization of reaction-diffusion PDEs with arbitrary levels of instability and arbitrarily long input delay is a challenging problem that was introduced and solved using *the backstepping method* for PDEs in [13]. The method involves stabilizing a hyperbolic (transport) PDE that cascades into the reaction-diffusion PDE.

The idea of the PDE backstepping [14], [15] is to use an invertible transformation (usually a Volterra-type transformation), coupled with a state change of variables, if needed, to transform the unstable cascade system into an easy-to-analyze system, called the target system, chosen to satisfy the desired stability property. Then, the stability property is transferred to the original cascade system via the inverse transformation. This method has been widely extended to a variety of parabolic systems (see [2], [4], [11], [23], [24], [30] and the references therein). In [4], for instance, exponential stabilization of a class of coupled reaction-diffusion PDEs with different input and output delays was solved using an observer-based boundary feedback law based on an invertible Fredholm backstepping transformation. An alternative method for stabilization of parabolic PDEs with input delay is the *modal decomposition* method (see [5], [22]). The method consists of splitting the unstable PDE into a stable infinite-dimensional part and a finite-dimensional unstable part. Then, using classical predictor approaches, the unstable finite-dimensional system is stabilized. Recently, this approach was applied in [9], [10] to construct a new finite-dimensional observer design for a class of parabolic PDEs, which in turn was used in [9], [10] to construct an observed-based control that stabilizes the PDE system.

Most of the aforementioned works provide only asymptotic or exponential convergences, yet in several applications (e.g., rendezvousing of multi-agents, spacecraft docking, tactical missile guidance, and in chemical, biological, or population (epidemiological) processes - where the feedback action may be considerably delayed by time-consuming chemical measurements or biological tests), where the transient process must occur within a finite given time, and delays need to be perfectly compensated, finite-in-time convergences are strongly desired.

B. Finite-in-time stabilization of PDEs with input delay

Finite-in-time convergence refers to several properties, with three standing out: i) finite-time convergence where the system's solutions converge to the equilibrium in a finite time that depends on the initial conditions and may also depend on the system's parameter (see [1]). ii) fixed-time convergence where the finite time of convergence is uniformly bounded but

[1]Univ. Lyon, Université Claude Bernard Lyon 1, CNRS, LAGEPP UMR 5007, F-69100 Villeurbanne, France. (e-mail: salim.zekraoui@univ-lyon1.fr)

[2]CRIStAL UMR 9189 CNRS - Centre de Recherche en Informatique Signal et Automatique de Lille - CNRS, Centrale Lille, Univ. Lille, F-59000 Lille, France.

[3]Centrale Lille, F-59000 Lille, France.

[4]Department of Mechanical and Aerospace Engineering, University of California, San Diego, USA

may depend on some parameters of the system (see [20]). iii) Prescribed-time convergence where the time of convergence is arbitrarily chosen independently of the initial conditions and the system's parameters (see [25]) .

In the framework of finite-in-time stabilization of time-delay systems, very few results can be found even for finite-dimensional systems with input delay (e.g., [8], [17]–[19], [31], [32], [34]). Prescribed-time stabilization [25] and predictor feedback for compensation of input delay [14] are a perfect match because both techniques deal with finite-time dynamics. Intuitively, by applying predictor feedback to a prescribed-time feedback (for either an ODE or PDE plant), the former feedback being time-varying and the latter infinite-dimensional, one should be able to obtain convergence in a time that is the sum of the prescribed time and the input delay. And yet, already six years after [25], one can still find very few results that combine prescribed-time feedback with predictors.

In a notable exception from this slow progress, in [19], an ODE-PDE cascade representation of a class of LTI systems with input delay is provided and a time-varying backstepping-based approach is used to design a predictor feedback that ensures delay compensation in prescribed time. Recently, this approach has been extended to a class of one-dimensional reaction-diffusion PDE with boundary input delay in [26]. One of the striking features of time-varying prescribed-time controllers in both finite-dimensional and infinite dimensional settings, is not only that one can achieve convergence in desired time but also reduce state peaking during stabilization and reduce the control effort by distributing it more evenly over the time interval of convergence.

C. Contributions

In this paper, we address the problem of achieving prescribed-time boundary output-feedback stabilization for a class of one-dimensional linear reaction-diffusion partial differential equations (PDEs) with input delay. To solve this problem, we propose a novel approach, inspired by the employment of state predictions as represented in [14, Chapter 11], rather than the classical PDE backstepping given in [14, Chapter 18] for parabolic PDEs with input delay and rather than the time-varying PDE backstepping given in [26] for parabolic PDEs with input delay and in [31] for LTI systems with distributed input delay. This approach is an advantageous alternative that requires radical advancements to be adjusted from nonlinear ODEs to linear PDEs. Our approach is an extension of the results of [14, Chapter 11, page 171] on delay compensation for nonlinear ODEs with input delay, and the results of [32] on finite-time delay compensation for linear ODEs with input delay. Our contribution extends the results of [26] for the delay-dependent case to output-feedback stabilization.

The main idea of our approach is to transform the original parabolic PDE into a PDE-PDE cascade system and then apply only one time-varying backstepping transformation. Unlike [26] - where both the parabolic and hyperbolic parts of the cascade system are transformed using two different invertible backstepping transformations - we only transform the hyperbolic PDE state modeling the effect of the delay on the input. This transformation leads to a different target system composed of the studied parabolic system with a non-delayed new control input, coupled with a fixed-time vanishing transport equation. Since the coupling term can be treated in the stability analysis as an additive disturbances that vanishes after a certain finite time, the non-delayed new control input is designed based on the existing results related to prescribed-time full-state (resp. output-feedback) boundary stabilization of reaction-diffusion PDEs given in [6] (resp. [27]). Finally, by inverse transformation, the stability property and the desired finite-in-time convergence is transferred back to the original closed-loop system and the predictor-based controller is expressed in terms of the non-delayed new control input and the prediction variables.

Unlike the existing results on delay compensation, our formulation makes a clear distinction between the delay compensation task which aims to transform the delayed parabolic system into a disturbed version of the studied system with a non-delayed new control input, and the stabilization task which aims to design a stabilizing control for the disturbed version of the free-delay parabolic PDE. The control design task can be achieved either using the existing backstepping-based results as we did in this contribution or based on a different technique like Control Lyapunov function (CLF) technique as in [33]. Moreover, unlike [26], our resulting predictor-based controller does not depend on a spatial derivative of the state and overcomes also the issue of incompatibility of boundary conditions of kernel equations (which arises when considering point-wise damping term in the design) as observed in [26]. In the course of developing a methodology alternative to [19], [26], [27], we develop a number of technical innovations, located throughout the paper and its appendices, and usable in future works on predictor-based prescribed-time stabilization.

D. Organization

This paper is organized as follows. In Section II, we introduce the unstable one-dimensional reaction-diffusion system with boundary input delay. In Section III, we focus on the problem of prescribed-time stabilization of the original system using full-state feedback control, where we start by reformulating the system as a PDE-PDE cascade system; We use an invertible backstepping transformation to link the cascade systems to some well-chosen prescribed-time stable (in short **PTS**) target systems. We perform a stability analysis on the target systems. Then, by inverse transformation, we establish the boundedness of the state of the original systems and their convergence to the origin in a prescribed time using a suitable norm equivalence. In Section IV, we switch to the problem of prescribed-time output-feedback stabilization, where we adapt our approach to taking into account the dynamics of the proposed observer system. In Section V, we consider a numerical example to illustrate the main results. Finally, conclusions and perspectives are given in Section VI.

Notation:

$\mathbb{R}_+$ denotes the set of non negative real numbers. $\mathbb{N}^*$ denotes the set of natural numbers excluding zero. For all $a, b \in \mathbb{R}$

with $a \leq b$, $L^2(a,b)$ denotes the set $\{f : [a,b] \to \mathbb{R} : \int_a^b |f(x)|^2 dx < \infty\}$ with the scalar product $\langle f, g\rangle_{L^2(a,b)} := \int_a^b f(x)g(x)dx$ and the norm $\|f\|_{L^2(a,b)} := (\int_a^b f(x)^2 dx)^{\frac{1}{2}}$. For any $t_0 \geq 0$, $T > 0$, and $v : [t_0, t_0+T) \times [0,1] \to \mathbb{R}$, $v(t,\cdot) \in L^2(0,1)$ denotes the profile of v at a certain time $t \in [t_0, t_0+T)$. A function $\alpha : \mathbb{R}_+ \to \mathbb{R}_+$ is said to be a class-$\mathcal{K}$ function if it is continuous, zero at zero, and strictly increasing. A continuous function $\beta : \mathbb{R}_+ \times \mathbb{R}_+ \to \mathbb{R}_+$ belongs to the class-$\mathcal{KL}$ if $\beta(\cdot, t) \in \mathcal{K}$ for each fixed $t \in \mathbb{R}_+$, and $\beta(r,\cdot)$ is decreasing and $\lim_{t\to+\infty} \beta(r,t) = 0$ for each $r \in \mathbb{R}_+$.

II. PROBLEM STATEMENT

Let us consider the following reaction-diffusion equation with a constant reaction coefficient $\lambda \in \mathbb{R}$ and a known constant boundary input delay $D > 0$:

$$z_t(t,x) = z_{xx}(t,x) + \lambda z(t,x), \tag{1}$$
$$z(t,0) = 0, \tag{2}$$
$$z(t,1) = U(t-D), \tag{3}$$
$$Y(t) = z_x(t,1), \tag{4}$$
$$z(t_0,x) = z_0(x), \tag{5}$$

with the initial time $t_0 \geq 0$, the time and space variables $(t,x) \in [t_0, t_0+D+T) \times [0,1]$, the state $z(t,x) \in \mathbb{R}$, the control $U(t) \in \mathbb{R}$, with the following initial condition: $U(t_0+s) = 0$ for all $s \in [-D, 0]$, the collocated output $Y(t) \in \mathbb{R}$, and the initial condition $z_0 \in L^2(0,1)$.

Remark 1: Other configurations for the problem statement can be considered: for example, we can consider Dirichlet actuation $z(t,1) = U(t-D)$ with anti-collocated sensing $Y(t) = z_x(t,0)$, or Neumann actuation $z_x(t,1) = U(t-D)$ with anti-collocated sensing $Y(t) = z(t,0)$; however, we focus here on the simplest configuration in order to better and more pedagogically present our contribution.

Our main goal is to design a predictor-based output-feedback controller achieving prescribed-time stabilization of the closed-loop system (1)-(5) in the following sense: there exists a class-$\mathcal{KL}$ function β and a continuous function $\mu : [t_0, t_0+D+T) \to \mathbb{R}_+$, where μ tends to infinity as t goes to t_0+D+T, such that for any initial condition and for all $t \in [t_0, t_0+D+T)$, the following estimate holds: $\|z(t,\cdot)\|_{L^2(0,1)} \leq \beta\Big(\|z_0\|_{L^2(0,1)}, \mu(t-t_0-D)\Big)$.

In order to solve this problem we follow three steps:

- **Step 1:** Prescribed-time full-state feedback stabilization: we start by solving the problem of prescribed-time stabilization by full-state feedback of the closed-loop system (1)-(5). The idea is to first represent the input delay as a linear transport PDE (inspired from [13]), so that the system (1)-(5) is rewritten as a parabolic-transport hyperbolic PDE-PDE cascade system. Then, we propose a novel infinite-dimensional transformation (inspired from [14, Chapter 11, page 171]) to transform the resulting cascade system into a suitable target system that is prescribed-time stable (**PTS**). The target system is chosen to be a parabolic-transport hyperbolic PDE-PDE cascade system with diffusion dynamics being exactly as in (1) but whose Dirichlet right boundary condition is given not only in terms of a boundary term of the transport PDE which vanishes after delay D but includes also a feedback term which renders the diffusion PDE converging to zero after the delay. Such a feedback is borrowed from [6]. Finally, the stability property is transferred to (1)-(5) via the inverse transformation.
- **Step 2:** Prescribed-time observer design: We employ the prescribed-time observer design from [27] to estimate the states of (1)-(5) in a prescribed time.
- **Step 3:** Prescribed-time output-feedback stabilization: We combine the designed prescribed-time observer with the full-state control to ensure output-feedback stabilization in a prescribed time of the closed-loop system (1)-(5).

Remark 2: Extension of our result to the case of input-output delay

$$\bar{z}_t(t,x) = \bar{z}_{xx}(t,x) + \lambda \bar{z}(t,x), \tag{6}$$
$$\bar{z}(t,0) = 0, \tag{7}$$
$$\bar{z}(t,1) = U(t-D_1), \tag{8}$$
$$Y(t) = \bar{z}_x(t-D_2, 1), \tag{9}$$

is straightforward by using the following change of variables $z(t,x) = \bar{z}(t-D_2, x)$, as it allows to obtain a system of the form of (1)-(5) (with $D = D_1 + D_2$) for which we can apply our approach to ensure prescribed-time stabilization.

Remark 3: In our approach, it is necessary to have a prescribed-time boundary controller for the delay-free case of system (1)-(5). Therefore, we follow the prescribed-time boundary control design in [6] that we recall next.

III. PRESCRIBED-TIME STABILIZATION BY FULL-STATE FEEDBACK

A. Prescribed-time boundary stabilization in the delay-free case

Before presenting our approach, let us briefly summarize the main results of [6] on prescribed-time boundary stabilization of system (1)-(5) when $D = 0$. To that end, consider the following blow-up function:

$$\gamma_m(t-\bar{t}_0) := \frac{\gamma_{m,0}^m T^m}{(\bar{t}_0+T-t)^m}, \tag{10}$$

for $m \in \mathbb{N}^*$, defined for all $t \in [\bar{t}_0, \bar{t}_0+T)$ where $T > 0$ is a priori fixed.

We recall the following time-varying boundary control:

$$U(t) = \int_0^1 K(1,s,t-\bar{t}_0) z(t,s) ds, \tag{11}$$

where K is given explicitly in [6, Lemma 1] by

$$K(x,s,t-\bar{t}_0) = -\frac{1}{2}\gamma_2(t-\bar{t}_0)s\sum_{n=0}^{\infty}\frac{\left(\sqrt{\gamma_2(t-\bar{t}_0)}\right)^n}{(n+1)!} \times \left(\frac{x^2-s^2}{4T\gamma_{2,0}}\right)^n L_n^{(1)}\left(-T\gamma_{2,0}\sqrt{\gamma_2(t-\bar{t}_0)}\right), \tag{12}$$

where $L_n^{(1)}(\cdot)$ are the generalized Laguerre polynomials. In addition, (12) can be simplified using the first-order modified Bessel function $I_1(\cdot)$ to get

$$K(x,s,t-\bar{t}_0) = -\gamma_2(t-\bar{t}_0)s\, e^{\frac{\sqrt{\gamma_2(t-\bar{t}_0)}(x^2-s^2)}{4T\gamma_{2,0}}} \times \frac{I_1(\sqrt{\gamma_2(t-\bar{t}_0)(x^2-s^2)})}{\sqrt{\gamma_2(t-\bar{t}_0)(x^2-s^2)}}, \tag{13}$$

for $(x,s,t) \in \mathcal{T} := \{(x,s,t) \in [0,1]^2 \times [\bar{t}_0, \bar{t}_0+T) : s \le x\}$.

Making use of the controller (11)-(13), the closed-loop system (1)-(5) with $D = 0$ is **PTS** (see [6, Theorem 3]) provided that the control gain $\gamma_{2,0} = \gamma_2(0)$ satisfies

$$2\gamma_{2,0}T > 1. \tag{14}$$

More precisely, there exist positive constants $c_k,\ c_l > 0$, and $M > 0$ such that for any initial condition $z(\bar{t}_0,\cdot)$ at an initial time $\bar{t}_0$, we have

$$\|z(t,\cdot)\|_{L^2(0,1)} \le \xi_1(t-\bar{t}_0)\|z(\bar{t}_0,\cdot)\|_{L^2(0,1)}, \tag{15}$$

where

$$\xi_1(t-\bar{t}_0) := M\left(c_l\gamma_2(t-\bar{t}_0)e^{-\alpha_0\sqrt{\gamma_2(t-\bar{t}_0)}} + e^{-\gamma_{2,0}T\sqrt{\gamma_2(t-\bar{t}_0)}}\right), \tag{16}$$

with $M := e^{(\gamma_{2,0}^2+\lambda)T}\left(1+e^{\frac{1}{4T}+\gamma_{2,0}c_k}\right) > 0$ and $\alpha_0 := (4\gamma_{2,0}^2T^2-1)(4T\gamma_{2,0})^{-1} > 0$.

Furthermore, $U(t)$ satisfies

$$|U(t)| \le \xi_2(t-\bar{t}_0)\|z(\bar{t}_0,\cdot)\|_{L^2(0,1)}, \tag{17}$$

with

$$\xi_2(t-\bar{t}_0) := c_l M\gamma_2(t-\bar{t}_0)e^{-\alpha_0\sqrt{\gamma_2(t-\bar{t}_0)}}. \tag{18}$$

In particular, $\|z(t,\cdot)\|_{L^2(0,1)} \to 0$, and $|U(t)| \to 0$ when $t \to \bar{t}_0 + T$.

Remark 4: To achieve exponential stabilization, it is sufficient to replace the control gain K by

$$K_{\exp}(x,s) = -(\lambda+\lambda_0)s\frac{I_1(\sqrt{(\lambda+\lambda_0)(x^2-s^2)})}{\sqrt{(\lambda+\lambda_0)(x^2-s^2)}}, \tag{19}$$

for all $(x,s) \in \mathcal{T} := \{(x,s) \in [0,1]^2 : s \le x\}$ and any control gain $\lambda+\lambda_0 \ge 0$, with $\lambda_0 \ge 0$ a tuning parameter.

B. Prescribed-time stabilization for the input delay case

Let us now consider the PDE-PDE cascade representation of (1)-(5) given by

$$z_t(t,x) = z_{xx}(t,x) + \lambda z(t,x), \tag{20}$$
$$z(t,0) = 0, \tag{21}$$
$$z(t,1) = v(t,0), \tag{22}$$
$$v_t(t,y) = v_y(t,y), \tag{23}$$
$$v(t,D) = U(t), \tag{24}$$

with $(t,x,y) \in [t_0, t_0+D+T) \times [0,1] \times [0,D]$, and $v(t,\cdot)$ is the transport PDE state whose solution is given by

$$v(t,y) = \begin{cases} 0, & t_0 \le t+y \le t_0+D, \\ U(t+y-D), & t+y \ge t_0+D. \end{cases} \tag{25}$$

Note that the control's initial condition is taken, for simplicity, as $U(t_0+s) = 0$ for all $s \in [-D,0]$.

1) Time-varying infinite-dimensional backstepping transformation: Inspired by [14, Chapter 11, page 171], we propose the following time-varying infinite-dimensional backstepping transformation:

$$\omega(t,y) = v(t,y) - \mathscr{F}(t+y-t_0-D, \varphi(t,\cdot,y)), \tag{26}$$

where $\mathscr{F}$ is given by

$$\mathscr{F}(t+y-t_0-D,\varphi(t,\cdot,y)) := \int_0^1 K(1,s,t+y-t_0-D) \times \varphi(t,s,y)ds, \tag{27}$$

with K defined as in (13) (with $\bar{t}_0 = t_0+D$), and the predictor φ is chosen to satisfy $\varphi(t,x,y) = z(t+y,x)$ which means it is the solution of

$$\varphi_y(t,x,y) = \varphi_{xx}(t,x,y) + \lambda\varphi(t,x,y), \tag{28}$$
$$\varphi(t,0,y) = 0, \tag{29}$$
$$\varphi(t,1,y) = v(t,y), \tag{30}$$
$$\varphi(t,x,0) = z(t,x), \tag{31}$$

with $(t,x,y) \in \{(t,x,y) \in [t_0, t_0+D+T) \times [0,1] \times [0,D] : t+y \in [t_0+D, t_0+D+T)\}$.

Notice that φ can be computed explicitly (see [21, Chapter 3, page 266]) as follows:

$$\varphi(t,x,y) = 2\sum_{n=1}^{+\infty}\sin(n\pi x)e^{(\lambda-n^2\pi^2)y}\left[\int_0^1 \sin(n\pi s) \times z(t,s)ds + n\pi(-1)^{n+1}\int_0^y e^{-(\lambda-n^2\pi^2)\tau}v(t,\tau)d\tau\right] \tag{32}$$

$$= \int_0^1\left[2\sum_{n=1}^{+\infty}\sin(n\pi x)\sin(n\pi s)e^{(\lambda-n^2\pi^2)y}\right]z(t,s)ds + \int_0^y\left[2\pi\sum_{n=1}^{+\infty}n(-1)^{n+1}\sin(n\pi x)e^{(\lambda-n^2\pi^2)(y-\tau)}\right]v(t,\tau)d\tau, \tag{33}$$

Now, by substituting (32) in (26), we obtain,

$$\omega(t,y) = v(t,y) - \int_0^1 K(1,x,t+y-t_0-D)\varphi(t,x,y)dx \tag{34}$$

$$= v(t,y) - \int_0^1 K(1,x,t+y-t_0-D)\left(\int_0^1 \left[2\sum_{n=1}^{+\infty} \sin(n\pi x)\sin(n\pi s)e^{(\lambda-n^2\pi^2)y}\right] z(t,s)ds + \int_0^y [2\pi \times \sum_{n=1}^{+\infty} n(-1)^{n+1}\sin(n\pi x)e^{(\lambda-n^2\pi^2)(y-\tau)}\right] v(t,\tau)d\tau\Bigg) dx \tag{35}$$

$$= v(t,y) - \int_0^1 \left[2\sum_{n=1}^{+\infty}\sin(n\pi s)e^{(\lambda-n^2\pi^2)y} \times \int_0^1 K(1,x,t+y-t_0-D)\sin(n\pi x)dx\right] z(t,s)ds + \int_0^y \left[2\pi\sum_{n=1}^{+\infty} n(-1)^{n+1}e^{(\lambda-n^2\pi^2)(y-\tau)} \times \int_0^1 K(1,x,t+y-t_0-D)\sin(n\pi x)dx\right] v(t,\tau)d\tau \tag{36}$$

$$:= v(t,y) - \int_0^1 \bar{\gamma}_2(y,s,t+y-t_0-D)z(t,s)\ ds + \int_0^y \bar{q}(y-\tau,t+y-t_0-D)v(t,\tau)d\tau, \tag{37}$$

where the new kernels $\bar{\gamma}$ and $\bar{q}$ are given by

$$\bar{\gamma}(y,s,t+y-t_0-D) := 2\sum_{n=1}^{+\infty} e^{(\lambda-n^2\pi^2)y}\sin(n\pi s) \times \int_0^1 K(1,x,t+y-t_0-D)\sin(n\pi x)dx, \tag{38}$$

and

$$\bar{q}(y-\tau,t+y-t_0-D) := -2\pi\sum_{n=1}^{+\infty} e^{(\lambda-n^2\pi^2)(y-\tau)} \times n(-1)^{n+1}\int_0^1 K(1,x,t+y-t_0-D)\sin(n\pi x)dx, \tag{39}$$

Remark 5: To obtain exponential stabilization of (1)-(5), it is sufficient to replace the transformation (26) by

$$\omega(t,y) = v(t,y) - \mathscr{F}_{\text{exp}}(\varphi(t,\cdot,y)), \tag{40}$$

where φ is generated as before, i.e., from (28)-(31), and $\mathscr{F}_{\text{exp}}$ is defined as,

$$\mathscr{F}_{\text{exp}}(\varphi(t,\cdot,y)) := \int_0^1 K_{\text{exp}}(1,s)\varphi(t,s,y)ds, \tag{41}$$

with the gain K_{exp} given as in (19). Moreover, using (32), the transformation (26) can be simplified as follows:

$$\omega(t,y) = v(t,y) - \int_0^1 K_{\text{exp}}(1,x)\varphi(t,x,y)dx \tag{42}$$

$$= v(t,y) - \int_0^1 K_{\text{exp}}(1,x)\left(\int_0^1 \left[2\sum_{n=1}^{+\infty}\sin(n\pi x) \times \sin(n\pi s)e^{(\lambda-n^2\pi^2)y}\right] z(t,s)ds + \int_0^y \left[2\pi\sum_{n=1}^{+\infty} n \times(-1)^{n+1}\sin(n\pi x)e^{(\lambda-n^2\pi^2)(y-\tau)}\right] v(t,\tau)d\tau\right) dx \tag{43}$$

$$= v(t,y) - \int_0^1 \left[2\sum_{n=1}^{+\infty}\sin(n\pi s)e^{(\lambda-n^2\pi^2)y}\int_0^1 K_{\text{exp}}(1,x) \times \sin(n\pi x)dx\right] z(t,s)ds + \int_0^y \left[2\pi\sum_{n=1}^{+\infty} n(-1)^{n+1} \times e^{(\lambda-n^2\pi^2)(y-\tau)}\int_0^1 K_{\text{exp}}(1,x)\sin(n\pi x)dx\right] v(t,\tau)d\tau \tag{44}$$

$$:= \int_0^1 \bar{\gamma}_{\text{exp}}(y,s)z(t,s)\ ds + \int_0^y \bar{q}_{\text{exp}}(y-\tau)v(t,\tau)d\tau, \tag{45}$$

where the kernels $\bar{\gamma}_{\text{exp}}$ and $\bar{q}_{\text{exp}}$ are given by,

$$\bar{\gamma}_{\text{exp}}(y,s) := 2\sum_{n=1}^{+\infty} e^{(\lambda-n^2\pi^2)y}\sin(n\pi s) \times \int_0^1 K_{\text{exp}}(1,x)\sin(n\pi x)dx, \tag{46}$$

and

$$\bar{q}_{\text{exp}}(y-\tau) := -2\pi\sum_{n=1}^{+\infty} n(-1)^{n+1}e^{(\lambda-n^2\pi^2)(y-\tau)} \times \int_0^1 K_{\text{exp}}(1,x)\sin(n\pi x)dx, \tag{47}$$

hence, recovering the kernels of the backstepping transformation obtained in [13] for $\lambda_0 = 0$.

*2) **Target System** :* Next, using (26), we transform the system (20)-(24) into the following target system:

$$z_t(t,x) = z_{xx}(t,x) + \lambda z(t,x), \tag{48}$$
$$z(t,0) = 0, \tag{49}$$
$$z(t,1) = \omega(t,0) + \mathscr{F}(t-t_0-D,z(t,\cdot)), \tag{50}$$
$$\omega_t(t,y) = \omega_y(t,y), \tag{51}$$
$$\omega(t,D) = 0, \tag{52}$$

where $\omega : [t_0, t_0+D+T)\times[0,D] \to \mathbb{R}$ is the transport PDE state, and

$$\mathscr{F}(t-t_0-D,z(t,\cdot)) = \int_0^1 K(1,s,t-t_0-D)z(t,s)ds.$$

The transformation is realized by using the fact that $\varphi(t,x,y) = z(t+y,x)$ for all $(t,x,y) \in [t_0,t_0+D+T)\times[0,1]\times[0,D]$, and noticing that the time-varying transformation (26) satisfies (51) (i.e. $\omega_t(t,y) = \omega_y(t,y)$). Indeed, we

have

$$\omega_t(t,y) = v_t(t,y) - \frac{\partial \mathscr{F}(t+y-t_0-D,\varphi(t,\cdot,y))}{\partial t} \tag{53}$$

$$= v_y(t,y) - \int_0^1 \Big(K_t(1,s,t+y-t_0-D)\varphi(t,s,y) + K(1,s,t+y-t_0-D)\varphi_t(t,s,y) \Big) ds \tag{54}$$

$$= v_y(t,y) - \int_0^1 \Big(K_y(1,s,t+y-t_0-D)\varphi(t,s,y) + K(1,s,t+y-t_0-D)\varphi_y(t,s,y) \Big) ds \tag{55}$$

$$= v_y(t,y) - \frac{\partial \mathscr{F}(t+y-t_0-D,\varphi(t,\cdot,y))}{\partial y} \tag{56}$$

$$= \omega_y(t,y), \tag{57}$$

where we have used the fact that:

$$K_t(1,s,t+y-t_0-D) = \frac{\partial(t+y)}{\partial t}\frac{\partial K(1,s,t+y-t_0-D)}{\partial(t+y)} \tag{58}$$

$$= \frac{\partial K(1,s,t+y-t_0-D)}{\partial(t+y)} \tag{59}$$

$$= \frac{\partial(t+y)}{\partial y}\frac{\partial K(1,s,t+y-t_0-D)}{\partial(t+y)} \tag{60}$$

$$= K_y(1,s,t+y-t_0-D), \tag{61}$$

Remark 6: It is important to highlight the key feature of the chosen target system (48)-(52): when $t \geq t_0 + D$, $\omega(t,0)$ vanishes in (50); then, the resulting target system (48)-(50) with time-varying feedback $U(t) = \mathscr{F}(t-t_0-D, z(t,\cdot))$ converges in prescribed-time t_0+D+T to zero, in the light of the results introduced in III-A.

*3) **Time-varying infinite-dimensional inverse transformation**:* The inverse transformation is given by

$$v(t,y) = \omega(t,y) + \mathscr{F}(t+y-t_0-D,\psi(t,\cdot,y)), \tag{62}$$

with

$$\mathscr{F}(t+y-t_0-D,\psi(t,\cdot,y)) := \int_0^1 K(1,s,t+y-t_0-D) \times \psi(t,s,y)ds, \tag{63}$$

which, similarly as in (27), ψ is chosen to satisfy $\psi(t,x,y) = z(t+y,x)$. Consequently, ψ is the solution to

$$\psi_y(t,x,y) = \psi_{xx}(t,x,y) + \lambda\psi(t,x,y), \tag{64}$$

$$\psi(t,0,y) = 0, \tag{65}$$

$$\psi(t,1,y) = \omega(t,y) + \mathscr{F}(t+y-t_0-D,\psi(t,\cdot,y)), \tag{66}$$

$$\psi(t,x,0) = z(t,x). \tag{67}$$

Similarly to the direct transformation, we recover (23) (i.e. $v_t(t,y) = v_y(t,y)$) from the inverse transformation.

*4) **Prescribed-time predictor-based controller** :* Using (26) at $y = D$, we recover the expression of the boundary control $U(t)$ as follows

$$U(t) = v(t,D) = \mathscr{F}(t-t_0,\varphi(t,\cdot,D)) := \int_0^1 K(1,s,t-t_0)\varphi(t,s,D)ds, \tag{68}$$

where φ is the solution of (28)-(31) and K is given in (13). Equivalently, using (62) at $y = D$, we get

$$U(t) = v(t,D) = \mathscr{F}(t-t_0,\psi(t,\cdot,D)), \tag{69}$$

where ψ is the solution of (64)-(67).

From (38), the expression of the control $U(t)$ in (68) can be simplified as follows:

$$U(t) = \int_0^1 \bar{\gamma}(s,D,t-t_0)z(t,s)\ ds + \int_0^D \bar{q}(D-\tau,t-t_0)v(t,\tau)d\tau, \tag{70}$$

where $\bar{\gamma}$ and $\bar{q}$ are given in (38)-(39).

Remark 7: In light of Remarks 4 and 5, the expression of the control $U_{\text{exp}}(t)$ that achieves exponential stabilization of (1)-(5) is given as follows:

$$U_{\text{exp}}(t) = \int_0^1 \bar{\gamma}_{\text{exp}}(s,D)z(t,s)ds + \int_0^D \bar{q}_{\text{exp}}(D-\tau)v(t,\tau)d\tau, \tag{71}$$

where $\bar{\gamma}_{\text{exp}}$ and $\bar{q}_{\text{exp}}$ are given in (46) and (47), respectively.

*5) **Stability analysis**:* In this subsection, we start by performing the stability analysis on the target system (48)-(52). Then, by the inverse transformation (64)-(67) we establish the boundedness of the state of the original system (20)-(24) and its convergence to zero in a prescribed time using a suitable norm equivalence.

Proposition 1: Let $\gamma_{2,0}$ satisfy (14)*. There exists a polynomial function $Q(\cdot)$ in terms of $\gamma_2(t+y-t_0-D)$ such that, for all $t \in [t_0+D, t_0+D+T)$:*

$$\int_0^D \xi_2(t+y-t_0-D)^2 dy \leq Q\Big(2\alpha_0\sqrt{\gamma_2(t-t_0-D)}\Big) \times e^{-2\alpha_0\sqrt{\gamma_2(t-t_0-D)}}, \tag{72}$$

where ξ_2 is defined in (18)*.*

Proof: see Appendix I. ∎

Proposition 2: For the transport PDE $v(t,x)$ satisfying (23)*, the following estimates holds for $t \in [t_0+D, t_0+D+T)$:*

$$\|v(t,\cdot)\|_{L^2(0,D)} \leq \xi_3(t-t_0-D)\|z(t_0+D,\cdot)\|_{L^2(0,1)}, \tag{73}$$

where

$$\xi_3(t-t_0-D) := Q\Big(2\alpha_0\sqrt{\gamma_2(t-t_0-D)}\Big) \times e^{-2\alpha_0\sqrt{\gamma_2(t-t_0-D)}}. \tag{74}$$

where $Q(\cdot)$ is given as in Proposition 1. In particular, it holds $\|v(t,\cdot)\|_{L^2(0,D)} \to 0$ for all $t \to t_0 + D + T$.

Proof: From (62) and using the fact that $\omega(t,y) = 0, \forall (t,y) \in [t_0+D, t_0+D+T) \times [0,D]$, we recover that

$$v(t,y) = \mathscr{F}(t+y-t_0-D, \psi(t,\cdot,y)). \tag{75}$$

Next, by squaring the previous equality, using the fact that $\psi(t,\cdot,y) = z(t+y,\cdot)$, and using (17) for $\bar{t}_0 := t_0 + D$, we get,

$$|v(t,y)|^2 \leq \xi_2(t+y-t_0-D)^2 \|z(t_0+D,\cdot)\|^2_{L^2(0,1)}. \tag{76}$$

Now, by integrating from 0 to D with respect to y and using (72) in Proposition 1, we obtain,

$$\|v(t,\cdot)\|^2_{L^2(0,D)} \leq \int_0^D \xi_2(t+y-t_0-D)^2 dy \|z(t_0+D,\cdot)\|^2_{L^2(0,1)} \tag{77}$$

$$\leq \xi_3(t-t_0-D)\|z(t_0+D,\cdot)\|^2_{L^2(0,1)}, \tag{78}$$

where ξ_3 is given in (74).

Now, by passing to the square roots, we recover (73). In particular, we can clearly see that $\xi_3(t-t_0-D) \to 0$ as $t \to t_0+D+T$. As a result, we obtain that $\|v(t,\cdot)\|_{L^2(0,D)} \to 0$ when $t \to t_0+D+T$.

■

Let us now introduce our first main result.

Theorem 1: Let the control gain $\gamma_{2,0}$ be chosen such that (14) *is ensured. Let $T > 0$, $D > 0$ and $t_0 \geq 0$. Then, the solution of the closed-loop system* (20)-(24) *with the prescribed-time time-varying controller* (68) *(or* (69)*) is* ***PTS*** *in the following sense: For any initial condition z_0, the quantities $\|z(t,\cdot)\|_{L^2(0,1)}$ and $\|v(t,\cdot)\|_{L^2(0,D)}$ remain bounded for all $t \in [t_0, t_0+D]$; and for all $t \in [t_0+D, t_0+D+T)$, the following norm $I(t) = \|z(t,\cdot)\|_{L^2(0,1)} + \|v(t,\cdot)\|_{L^2(0,D)}$ satisfies,*

$$I(t) \leq \mathcal{B}_D \xi_4(t-t_0-D)\|z_0\|_{L^2(0,1)}, \tag{79}$$

with $\xi_4 = \xi_1 + \xi_3$ and $\mathcal{B}_D = 2e^{\lambda(t_0+D)}\left(e^{-\pi^2 t_0} + \frac{1}{2\sqrt{\pi t_0}}\right)$. In particular, $I(t) \to 0$ as $t \to t_0+D+T$ and $|U(t)| \to 0$ as $t \to t_0+T$.

Proof: • Boundedness of the norm $\|z(t,\cdot)\|_{L^2(1,0)}$ in $[t_0, t_0+D]$:

Using the fact that $v(t,0) = U(t-D) = 0$ for all $t \in [t_0, t_0+D]$, the solution of (20)-(24) is given explicitly from [21, Chapter 3] by

$$z(t,x) = 2\sum_{n=1}^{+\infty} e^{(\lambda - n^2\pi^2)t}\sin(n\pi x)\int_0^1 \sin(n\pi y) z_0(y) dy. \tag{80}$$

Then, we have

$$|z(t,x)| \leq 2\sum_{n=1}^{+\infty} e^{(\lambda-n^2\pi^2)t}|\sin(n\pi x)| \times \int_0^1 |\sin(n\pi y)||z_0(y)|\, dy \tag{81}$$

$$\leq 2\int_0^1 |z_0(y)|\, dy\; e^{\lambda t}\sum_{n=1}^{+\infty} e^{-n^2\pi^2 t}. \tag{82}$$

Next, using the Cauchy-Schwartz inequality, we obtain

$$|z(t,x)| \leq 2\|z_0\|_{L^2(0,1)} e^{\lambda t}\sum_{n=1}^{+\infty} e^{-n^2\pi^2 t}. \tag{83}$$

Now, using the fact that $t \in (t_0, t_0+D]$ and the fact that $\sum_{n=1}^{+\infty} e^{-n^2\pi^2 t}$ is a convergent series, we obtain

$$|z(t,x)| \leq 2\|z_0\|_{L^2(0,1)} e^{\lambda(t_0+D)}\sum_{n=1}^{+\infty} e^{-n^2\pi^2 t_0} \tag{84}$$

$$\leq 2\|z_0\|_{L^2(0,1)} e^{\lambda(t_0+D)}\left(e^{-\pi^2 t_0} + \int_1^{+\infty} e^{-x^2\pi^2 t_0} dx\right) \tag{85}$$

$$\leq 2\|z_0\|_{L^2(0,1)} e^{\lambda(t_0+D)}\left(e^{-\pi^2 t_0} + \int_0^{+\infty} e^{-x^2\pi^2 t_0} dx\right) \tag{86}$$

$$= 2\|z_0\|_{L^2(0,1)} e^{\lambda(t_0+D)}\left(e^{-\pi^2 t_0} + \frac{1}{2\sqrt{\pi t_0}}\right). \tag{87}$$

Finally, by squaring and integrating with respect to the variable x from 0 to 1, we get, for all $t \in [t_0, t_0+D]$

$$\|z(t,\cdot)\|_{L^2(0,1)} \leq \mathcal{B}_D \|z_0\|_{L^2(0,1)}, \tag{88}$$

with $\mathcal{B}_D := 2\|z_0\|_{L^2(0,1)} e^{\lambda(t_0+D)}\left(e^{-\pi^2 t_0} + \frac{1}{2\sqrt{\pi t_0}}\right)$.

• **PTS** of the closed-loop system of (20)-(24):
Using (15) and (73) from Proposition 2, we have

$$I(t) = \|z(t,\cdot)\|_{L^2(0,1)} + \|v(t,\cdot)\|_{L^2(0,D)} \tag{89}$$

$$\leq \xi_1(t-t_0-D)\|z(t_0+D,\cdot)\|_{L^2(0,1)} + \xi_3(t-t_0-D)\|z(t_0+D,\cdot)\|_{L^2(0,1)} \tag{90}$$

$$= \xi_4(t-t_0-D)\|z(t_0+D,\cdot)\|_{L^2(0,1)}, \tag{91}$$

for all $t \in [t_0+D, t_0+D+T)$, where $\xi_4(\cdot) := \xi_1(\cdot) + \xi_3(\cdot)$.

Next, using inequality (88) for $t = t_0+D$, we recover (79). In particular, we have that $I(t) \to 0$ when $t \to t_0+D+T$. Furthermore, we deduce that $\|z(t,\cdot)\|_{L^2(0,1)}$ is bounded for all $t \in [t_0, t_0+D+T)$.

• Boundedness of $\|v(t,\cdot)\|_{L^2(0,D)}$ in $[t_0, t_0+D]$:
Notice that v is given in $[t_0, t_0+D] \times [0,D]$ by

$$v(t,y) = \begin{cases} 0, & t \in [t_0, t_0+D-y], \\ U(t+y-D), & t \in [t_0+D-y, t_0+D]. \end{cases} \tag{92}$$

Thus, for all $(t,y)\in[t_0,t_0+D]\times[0,D]$, we have

$$|v(t,y)|\leq|U(t+y-D)|. \tag{93}$$

Next, by squaring the previous inequality, integrating w.r.t. y from 0 to D, and using Cauchy-Schwartz's inequality, we get

$$\|v(t,\cdot)\|^2_{L^2(0,D)}\leq\int_0^D|U(t+y-D)|^2dy \tag{94}$$

$$=\int_0^D|\mathscr{F}(t+y-t_0-D,\psi(t,\cdot,y))|^2dy \tag{95}$$

$$=\int_0^D\left(\int_0^1K(1,s,t+y-t_0-D)\psi(t,s,y)\,ds\right)^2dy \tag{96}$$

$$\leq\int_0^D\|K(1,\cdot,t+y-t_0-D)\|^2_{L^2(0,1)}\|\psi(t,\cdot,y)\|^2_{L^2(0,1)}dy \tag{97}$$

$$=\int_0^D\|K(1,\cdot,t+y-t_0-D)\|^2_{L^2(0,1)}\|z(t+y,\cdot)\|^2_{L^2(0,1)}dy. \tag{98}$$

Seeing that $\|z(t,\cdot)\|_{L^2(0,1)}$ is bounded for all $t\in[t_0,t_0+D+T)$ and that $\|K(1,\cdot,t+y-t_0-D)\|_{L^2(0,1)}$ is bounded in $[t_0,t_0+D]$, we deduce that $\|v(t,\cdot)\|_{L^2(0,D)}$ is bounded for all $t\in[t_0,t_0+D]$.

• Convergence of the control to the origin in a prescribed time:
From the equations (69) and (76), we have for all $t\geq t_0+D$

$$|U(t)|=|\mathscr{F}(t-t_0,\psi(t,\cdot,D))| \tag{99}$$

$$\leq\xi_2(t-t_0)\|z(t_0+D,\cdot)\|_{L^2(0,1)}. \tag{100}$$

In particular, it is clear that $U(t)\to0$ when $t\to t_0+T$. This concludes the proof. ■

IV. Prescribed-time stabilization by output feedback

Following the same lines of Section III, let us adapt our approach to design an observed-based control of (68).

A. Prescribed-time output boundary feedback stabilization in the delay-free case

As before, it is necessary to have a prescribed-time output-feedback boundary controller for the delay-free case of system (1)-(5). This can be achieved using [27] as summarized in what follows:

*1) **Observer design**:* Assume that $D=0$. The following observer system was proposed in [27]:

$$\hat{z}_t(t,x)=\hat{z}_{xx}(t,x)+\lambda\hat{z}(t,x)+P(x,t-\bar{t}_0,T)\times[z_x(t,1)-\hat{z}_x(t,1)], \tag{101}$$

$$\hat{z}(t,0)=0, \tag{102}$$

$$\hat{z}(t,1)=U(t), \tag{103}$$

$$\hat{z}(\bar{t}_0,x)=\hat{z}_0(x), \tag{104}$$

with observer gain P given by

$$P(x,t-\bar{t}_0,T):=-\frac{\gamma_3(t-\bar{t}_0)}{2\gamma_{3,0}^2}x\sum_{n=0}^{+\infty}\left(\frac{\gamma_3(t-\bar{t}_0)^{\frac{1}{3}}}{4T\gamma_{3,0}^{\frac{1}{3}}}\right)^n\times\frac{(-(1-x^2))^n}{(n+1)!}\sum_{j=0}^n\sum_{k=0}^j\frac{1}{j!}\binom{j}{k}\times\binom{n+2+k}{n-j}\left(\frac{-T\gamma_3(t-\bar{t}_0)^{\frac{2}{3}}}{2\gamma_{3,0}}\right)^j, \tag{105}$$

and γ_3 defined in (10). The observer state $\hat{z}(t,\cdot)$ converges to $z(t,\cdot)$ within the prescribed terminal time $\bar{t}_0+T$ provided that the observer gain $\gamma_{3,0}=\gamma_3(0)$ satisfies

$$\gamma_{3,0}T>\sqrt[3]{4}. \tag{106}$$

More precisely, there exist a positive constant α_1 and a positive polynomial function $Q_1(\cdot)$ in terms of $\gamma_2(t-\bar{t}_0)$ such that, for any initial conditions $z(\bar{t}_0,\cdot)$ and $\hat{z}(\bar{t}_0,\cdot)$, the following inequality holds for all $t\in[\bar{t}_0,\bar{t}_0+T)$:

$$\|z(t,\cdot)-\hat{z}(t,\cdot)\|_{L^2(0,1)}\leq\zeta_1(t-\bar{t}_0)\|z(\bar{t}_0,\cdot)-\hat{z}(\bar{t}_0,\cdot)\|_{L^2(0,1)}, \tag{107}$$

where

$$\zeta_1(t-\bar{t}_0):=Q_1\big(\alpha_1\gamma_2(t-\bar{t}_0)\big)e^{-\alpha_1\gamma_2(t-\bar{t}_0)}. \tag{108}$$

In particular, $\|z(t,\cdot)-\hat{z}(t,\cdot)\|_{L^2(0,1)}\to0$ as $t\to\bar{t}_0+T$.

*2) **Control design**:* We recall the following time-varying boundary output control:

$$U(t):=\int_0^1K(1,s,t-\bar{t}_0)\hat{z}(t,s)ds, \tag{109}$$

where the control gain K is as in (13) (subject to (14)) and $\hat{z}(t,\cdot)$ is generated from (101)-(104).

Using the control (109), the closed-loop system (1)-(5) is **PTS** in the following sense: there exist two positive constants α_2 and α_3 and two positive polynomial functions $Q_2(\cdot)$ and $Q_3(\cdot)$ defined in terms of $\gamma_1(t-\bar{t}_0)$ such that for any for any initial conditions $z(\bar{t}_0,\cdot)$ and $\hat{z}(\bar{t}_0,\cdot)$ at initial time $\bar{t}_0$, the following inequality holds:

$$\|z(t,\cdot)\|_{L^2(0,1)}+\|\hat{z}(t,\cdot)\|_{L^2(0,1)}\leq\zeta_2(t-\bar{t}_0)\left(\|z(\bar{t}_0,\cdot)\|_{L^2(0,1)}+\|\hat{z}(\bar{t}_0,\cdot)\|_{L^2(0,1)}\right), \tag{110}$$

for all $t\in[\bar{t}_0,\bar{t}_0+T)$, where

$$\zeta_2(t-\bar{t}_0):=Q_2\big(\alpha_2\gamma_1(t-\bar{t}_0)\big)e^{-\alpha_2\gamma_1(t-\bar{t}_0)}. \tag{111}$$

Furthermore, we have

$$|U(t)|\leq\zeta_3(t-\bar{t}_0)\|\hat{z}(\bar{t}_0,\cdot)\|_{L^2(0,1)}, \tag{112}$$

for all $t\in[\bar{t}_0,\bar{t}_0+T)$, with

$$\zeta_3(t-\bar{t}_0):=Q_3\big(\alpha_3\gamma_1(t-\bar{t}_0)\big)e^{-\alpha_3\gamma_1(t-\bar{t}_0)}. \tag{113}$$

In particular, $\|\hat{z}(t,\cdot)\|_{L^2(0,1)}\to0$, $\|z(t,\cdot)\|_{L^2(0,1)}\to0$, and $|U(t)|\to0$ when $t\to\bar{t}_0+T$.

B. Prescribed-time output boundary feedback stabilization for the input delay case

Let us now come back to (1)-(5) and its PDE-PDE cascade representation (20)-(24) with collocated output $Y(t) = z_x(t,1)$. We propose the following observer for (1)-(5):

$$\hat{z}_t(t,x) = \hat{z}_{xx}(t,x) + \lambda\hat{z}(t,x) + P(x,t-t_0,D+T) \times [z_x(t,1) - \hat{z}_x(t,1)], \quad (114)$$
$$\hat{z}(t,0) = 0, \quad (115)$$
$$\hat{z}(t,1) = v(t,0), \quad (116)$$
$$v_t(t,y) = v_y(t,y), \quad (117)$$
$$v(t,D) = U(t), \quad (118)$$

with the observer gain P is given as in (105) where we replace T by $D+T$ in the expression of $\gamma_3(t-t_0)$ to ensure that the convergence of $\hat{z}(t,\cdot)$ to $z(t,\cdot)$ is achieved in t_0+D+T instead of t_0+T. The transport PDE (117)-(118) is exactly as in (23)-(24), and notice that (116) can be always expressed using the delayed input $U(t-D)$ (i.e. $\hat{z}(t,1) = U(t-D)$).

Remark 8: Since our goal is to design an output-feedback control $U(t)$ for (20)-(24), we do not need to estimate the dynamics v of (117)-(118) (or (23)-(24)) because, from (25), it is expressed in terms of the control $U(t)$ and its delayed version $U(t-D)$ which in turn are expressed in terms of the observer state $\hat{z}(t,x)$. Consequently, the error system will be independent of the control input $U(t)$ and the transport state $v(t,y)$ and can be proven to be **PTS**, due to [27], regardless of the value of the delay D, if the observer gain $\gamma_{3,0} = \gamma_3(0)$ satisfies

$$\gamma_{3,0}(D+T) > \sqrt[3]{4}. \quad (119)$$

Thus, from (107), the following inequality holds:

$$\|z(t,\cdot) - \hat{z}(t,\cdot)\|_{L^2(0,1)} \leq \zeta_1(t-t_0-D)\|z_0 - \hat{z}_0\|_{L^2(0,1)}, \quad (120)$$

for $t \in [t_0, t_0+D+T)$ where $z_0 = z(t_0,\cdot)$ and $\hat{z}_0 = \hat{z}(t_0,\cdot)$. In particular, $\|z(t,\cdot)\|_{L^2(0,1)} \to \|\hat{z}(t,\cdot)\|_{L^2(0,1)}$ as $t \to t_0 + D + T$.

1) Time-varying infinite-dimensional backstepping transformation: As in Subsection III-B.1, we consider the following time-varying infinite-dimensional backstepping transformation:

$$\omega(t,y) = v(t,y) - \mathscr{F}(t+y-t_0-D, \hat{\varphi}(t,\cdot,y)), \quad (121)$$

where $\mathscr{F}$ has the same structure as in (27), i.e.,

$$\mathscr{F}(t+y-t_0-D, \hat{\varphi}(t,\cdot,y)) := \int_0^1 K(1,s,t+y-t_0-D) \times \hat{\varphi}(t,s,y)ds, \quad (122)$$

and $\hat{\varphi}$ is chosen to satisfy $\hat{\varphi}(t,x,y) = \hat{z}(t+y,x)$, and therefore, is solution of the following parabolic PDE:

$$\hat{\varphi}_y(t,x,y) = \hat{\varphi}_{xx}(t,x,y) + \lambda\hat{\varphi}(t,x,y) + P(x,t+y-t_0,D+T) \times [\varphi_x(t,1,y) - \hat{\varphi}_x(t,1,y)], \quad (123)$$
$$\hat{\varphi}(t,0,y) = 0, \quad (124)$$
$$\hat{\varphi}(t,1,y) = v(t,y), \quad (125)$$
$$\hat{\varphi}(t,x,0) = \hat{z}(t,x), \quad (126)$$

with φ being generated from (28)-(31).

2) Target System : Using (121), we transform respectively (20)-(24) and (114)-(116) into the two following target systems:

$$z_t(t,x) = z_{xx}(t,x) + \lambda z(t,x), \quad (127)$$
$$z(t,0) = 0, \quad (128)$$
$$z(t,1) = \omega(t,0) + \mathscr{F}(t-t_0-D, \hat{z}(t,\cdot)), \quad (129)$$
$$\omega_t(t,y) = \omega_y(t,y), \quad (130)$$
$$\omega(t,D) = 0, \quad (131)$$

and

$$\hat{z}_t(t,x) = \hat{z}_{xx}(t,x) + \lambda\hat{z}(t,x) + P(x,t-t_0,D+T) \times [z_x(t,1) - \hat{z}_x(t,1)], \quad (132)$$
$$\hat{z}(t,0) = 0, \quad (133)$$
$$\hat{z}(t,1) = \omega(t,0) + \mathscr{F}(t-t_0-D, \hat{z}(t,\cdot)), \quad (134)$$

where $\omega : [t_0, t_0+D+T) \times [0,D] \to \mathbb{R}$ is the transport PDE state.

Note that using the fact that $\varphi(t,x,y) = z(t+y,x)$ and $\hat{\varphi}(t,x,y) = \hat{z}(t+y,x)$ for all $(t,x,y) \in [t_0, t_0+D+T) \times [0,1] \times [0,D]$, it is clear that (121) verifies (130)-(131).

3) Time-varying infinite-dimensional inverse transformation: The inverse transformation is given by,

$$v(t,y) = \omega(t,y) + \mathscr{F}(t+y-t_0-D, \hat{\psi}(t,\cdot,y)), \quad (135)$$

where

$$\mathscr{F}(t+y-t_0-D, \hat{\psi}(t,\cdot,y)) := \int_0^1 K(1,s,t+y-t_0-D) \times \hat{\psi}(t,s,y)ds, \quad (136)$$

where $\hat{\psi}$ is the solution of

$$\hat{\psi}_y(t,x,y) = \hat{\psi}_{xx}(t,x,y) + \lambda\hat{\psi}(t,x,y) + P(x,t+y-t_0,D+T) \times \left[\psi_x(t,1,y) - \hat{\psi}_x(t,1,y)\right], \quad (137)$$
$$\hat{\psi}(t,0,y) = 0, \quad (138)$$
$$\hat{\psi}(t,1,y) = \omega(t,y) + \mathscr{F}(t+y-t_0-D, \hat{\psi}(t,\cdot,y)), \quad (139)$$
$$\hat{\psi}(t,x,0) = \hat{z}(t,x), \quad (140)$$

and ψ is generated from

$$\psi_y(t,x,y) = \psi_{xx}(t,x,y) + \lambda\psi(t,x,y), \quad (141)$$
$$\psi(t,0,y) = 0, \quad (142)$$
$$\psi(t,1,y) = \omega(t,y) + \mathscr{F}(t+y-t_0-D, \hat{\psi}(t,\cdot,y)), \quad (143)$$
$$\psi(t,x,0) = z(t,x). \quad (144)$$

Similarly, from the inverse transformation (135), we recover (23)-(24).

*4) **Prescribed-time predictor-based output controller** :* As in Subsection III-B.4, we recover the expression of the boundary control $U(t)$ as follows:

$$U(t) = v(t,D) = \mathscr{F}(t-t_0, \hat{\varphi}(t,\cdot,D)) := \int_0^1 K(1,s,t-t_0)\hat{\varphi}(t,s,D)ds, \quad (145)$$

from (121) at $y = D$, where $\hat{\varphi}$ is generated from (28)-(31) and K is given in (13). Likewise from (135) at $y = D$, we can get

$$U(t) = v(t,D) = \mathscr{F}(t-t_0, \hat{\psi}(t,\cdot,D)), \quad (146)$$

where $\hat{\psi}$ is generated from (137)-(140).

Remark 9: To achieve exponential output-feedback stabilization, it is sufficient to replace the control gain K by K_{exp} in (19) as in Remark 5 and the observer gain P by

$$P_{\text{exp}}(x) = -(\lambda+\lambda_0)x\frac{I_1(\sqrt{(\lambda+\lambda_0)(1-x^2)})}{\sqrt{(\lambda+\lambda_0)(1-x^2)}}, \quad (147)$$

for all $x \in [0,1]$ and any observer gain $\lambda + \lambda_0 \geq 0$, with $\lambda_0 \geq 0$ a tuning parameter. The expression of the exponential predictor-based output-feedback controller $U_{\text{exp}}(t)$ is then given by

$$U_{\text{exp}}(t) = \int_0^1 K_{\text{exp}}(1,s)\hat{\varphi}(t,s,D)ds, \quad (148)$$

or

$$U_{\text{exp}}(t) = \int_0^1 K_{\text{exp}}(1,s)\hat{\psi}(t,s,D)ds, \quad (149)$$

with $\hat{\varphi}$ and $\hat{\psi}$ are respectively generated from (123)-(126) and (137)-(140) using the observer gain $P_{\text{exp}}(x)$ (147).

*5) **Stability analysis**:* In this subsection, we start by performing a stability analysis on the target system (127)-(131). Then, by the inverse transformation (135), we establish the boundedness of the state of the original system (20)-(24) and its convergence to zero in a prescribed time using a suitable norm equivalence.

Proposition 3: Let the control and observer gains $\gamma_{2,0}$ and $\gamma_{3,0}$ satisfy (14) *and* (119) *respectively. Then, there exists a rational function $Q_4(\cdot)$ in terms of $\gamma_1(t-t_0-D)$ such that,*

$$\int_0^D \zeta_3(t+y-t_0-D)^2dy \leq Q_4(\alpha_3\gamma_1(t-t_0-D)) \times e^{-\alpha_3\gamma_1(t-t_0-D)}, \quad (150)$$

where $\gamma_1(\cdot)$ and $\zeta_3(\cdot)$ given in (10) *and* (113) *respectively.*

Proof: see Appendix II. ∎

Proposition 4: For the transport PDE $v(t,x)$ satisfying (23)*, there exists a positive polynomial function $Q_4(\cdot)$ in terms of $\gamma_1(t-t_0-D)$ such that the following estimate holds for $t \in [t_0+D, t_0+D+T)$:*

$$\|v(t,\cdot)\|_{L^2(0,D)} \leq \zeta_4(t-t_0-D)\left(\|z(t_0+D,\cdot)\|_{L^2(0,1)} + \|\hat{z}(t_0+D,\cdot)\|_{L^2(0,1)}\right), \quad (151)$$

where

$$\zeta_4(t-t_0-D) := Q_4(\alpha_3\gamma_1(t+y-t_0-D))e^{-\alpha_3\gamma_1(t+y-t_0-D)},$$

with $\gamma_1(\cdot)$ given in (10)*. In particular, it holds $\|v(t,\cdot)\|_{L^2(0,D)} \to 0$ for all $t \to t_0+D+T$.*

Proof: Let $t \in [t_0+D, t_0+D+T)$. Then, from (135) and using the fact that $\omega(t,y) = 0, \forall (t,y) \in [t_0+D, t_0+D+T) \times [0,D]$, we recover

$$v(t,y) = \mathscr{F}(t+y-t_0-D, \hat{\psi}(t,\cdot,y)). \quad (152)$$

Next, by squaring the previous equality and using the fact that $\hat{\psi}(t,\cdot,y) = \hat{z}(t+y,\cdot)$ and using (112) for $\bar{t}_0 := t_0+D$, we obtain,

$$|v(t,y)|^2 \leq \zeta_3(t+y-t_0-D)^2\left(\|z(t_0+D,\cdot)\|_{L^2(0,1)} + \|\hat{z}(t_0+D,\cdot)\|_{L^2(0,1)}\right)^2. \quad (153)$$

Now, by integrating from 0 to D with respect to y and using (150) in Proposition 3, we obtain,

$$\|v(t,\cdot)\|^2_{L^2(0,D)} \leq \int_0^D \zeta_3(t+y-t_0-D)^2dy \times \left(\|z(t_0+D,\cdot)\|_{L^2(0,1)} + \|\hat{z}(t_0+D,\cdot)\|_{L^2(0,1)}\right)^2 \quad (154)$$

$$\leq \zeta_4(t-t_0-D)\left(\|z(t_0+D,\cdot)\|_{L^2(0,1)} + \|\hat{z}(t_0+D,\cdot)\|_{L^2(0,1)}\right)^2, \quad (155)$$

where

$$\zeta_4(t-t_0-D) := Q_4(\alpha_3\gamma_1(t-t_0-D))e^{-\alpha_3\gamma_1(t-t_0-D)}. \quad (156)$$

Finally, by passing to the square roots,

$$\|v(t,\cdot)\|_{L^2(0,D)} \leq \zeta_4(t-t_0-D)\left(\|z(t_0+D,\cdot)\|_{L^2(0,1)} + \|\hat{z}(t_0+D,\cdot)\|_{L^2(0,1)}\right). \quad (157)$$

In particular, we get $\|v(t,\cdot)\|_{L^2(0,D)} \to 0$ as $t \to t_0+D+T$. ∎

Let us now give our second main result,

Theorem 2: Let the control and observer gains $\gamma_{2,0}$ and $\gamma_{3,0}$ be chosen such that (14) *and* (119) *are ensured. Let $T > 0$, $D > 0$ and $t_0 \geq 0$. Then, the solution of the closed-loop system* (20)-(24) *with the observer* (114)-(116) *and the prescribed-time time-varying output control* (145) *(or* (146)*) is **PTS** in the following sense: For any initial conditions z_0 and $\hat{z}_0$, the quantities $\|z(t,\cdot)\|_{L^2(0,1)}$, $\|\hat{z}(t,\cdot)\|_{L^2(0,1)}$, and $\|v(t,\cdot)\|_{L^2(0,D)}$ remain bounded for all $t \in [t_0, t_0+D]$; and for all $t \in [t_0+D, t_0+D+T)$, the following norm $J(t) = \|z(t,\cdot)\|_{L^2(0,1)} + \|\hat{z}(t,\cdot)\|_{L^2(0,1)} + \|v(t,\cdot)\|_{L^2(0,D)}$ satisfies,*

$$J(t) \leq L_D\zeta_5(t-t_0-D)\left(\|z_0\|_{L^2(0,1)} + \|\hat{z}_0\|_{L^2(0,1)}\right), \quad (158)$$

where $\zeta_5(\cdot) := \zeta_2(\cdot) + \zeta_4(\cdot)$, $L_D := (\mathcal{B}_D + \bar{\mathcal{B}}_D) > 0$, $\mathcal{B}_D := 2e^{\lambda(t_0+D)}\left(e^{-\pi^2 t_0} + \frac{1}{2\sqrt{\pi t_0}}\right)$ and $\bar{\mathcal{B}}_D := \mathcal{B}_D + \sup_{s\in[t_0,t_0+D]} \zeta_1(s-t_0-D)$. In particular, $J(t) \to 0$ as $t \to t_0+D+T$ and $|U(t)| \to 0$ as $t \to t_0+T$.

Proof: • Boundedness of the two norms $\|z(t,\cdot)\|_{L^2(1,0)}$ and $\|\hat{z}(t,\cdot)\|_{L^2(1,0)}$ in $[t_0, t_0+D]$:

As in the proof of Theorem 1, it is clear that:

$$\|z(t,\cdot)\|_{L^2(0,1)} \leq \mathcal{B}_D \|z_0\|_{L^2(0,1)} \tag{159}$$
$$\leq \mathcal{B}_D(\|z_0\|_{L^2(0,1)} + \|\hat{z}_0\|_{L^2(0,1)}), \tag{160}$$

in $[t_0, t_0+D]$, with $\mathcal{B}_D = 2e^{\lambda(t_0+D)}\left(e^{-\pi^2 t_0} + \frac{1}{2\sqrt{\pi t_0}}\right)$.

Moreover, using (120) and (160), we obtain

$$\|\hat{z}(t,\cdot)\|_{L^2(0,1)} \leq \|z(t,\cdot)\|_{L^2(0,1)} + \|z(t,\cdot) - \hat{z}(t,\cdot)\|_{L^2(0,1)} \tag{161}$$
$$\leq \mathcal{B}_D(\|z_0\|_{L^2(0,1)} + \|\hat{z}_0\|_{L^2(0,1)}) + \zeta_1(t-t_0-D)\|z_0 - \hat{z}_0\|_{L^2(0,1)} \tag{162}$$
$$\leq \bar{\mathcal{B}}_D(\|z_0\|_{L^2(0,1)} + \|\hat{z}_0\|_{L^2(0,1)}). \tag{163}$$

with $\bar{\mathcal{B}}_D := \mathcal{B}_D + \sup_{s\in[t_0,t_0+D]} \zeta_1(s-t_0-D)$.

• **PTS** of the closed-loop system of (20)-(24):
Using (110) and (151) from Proposition 4, we have

$$J(t) = \|z(t,\cdot)\|_{L^2(0,1)} + \|\hat{z}(t,\cdot)\|_{L^2(0,1)} + \|v(t,\cdot)\|_{L^2(0,D)} \tag{164}$$
$$\leq \zeta_2(t-t_0-D)\left(\|z(t_0+D,\cdot)\|_{L^2(0,1)} + \|\hat{z}(t_0+D,\cdot)\|_{L^2(0,1)}\right) + \zeta_4(t-t_0-D) \times \left(\|z(t_0+D,\cdot)\|_{L^2(0,1)} + \|\hat{z}(t_0+D,\cdot)\|_{L^2(0,1)}\right) \tag{165}$$
$$= \zeta_5(t-t_0-D)\left(\|z(t_0+D,\cdot)\|_{L^2(0,1)} + \|\hat{z}(t_0+D,\cdot)\|_{L^2(0,1)}\right), \tag{166}$$

for all $t \in [t_0+D, t_0+D+T)$, where $\zeta_5(\cdot) := \zeta_2(\cdot) + \zeta_4(\cdot)$. Next, using (160) and (163) for $t = t_0 + D$, we recover (158). In particular, we have that $J(t) \to 0$ when $t \to t_0+D+T$. Furthermore, we deduce that $\|z(t,\cdot)\|_{L^2(0,1)}$ and $\|\hat{z}(t,\cdot)\|_{L^2(0,1)}$ are bounded for all $t \in [t_0, t_0+D+T)$.

• Boundedness of $\|v(t,\cdot)\|_{L^2(0,D)}$ in $[t_0, t_0+D]$:

Notice that v is given in $[t_0, t_0+D]\times[0,D]$ by

$$v(t,y) = \begin{cases} 0, & t \in [t_0, t_0+D-y], \\ U(t+y-D), & t \in [t_0+D-y, t_0+D]. \end{cases} \tag{167}$$

Thus, for all $(t,y) \in [t_0, t_0+D]\times[0,D]$, we have

$$|v(t,y)| \leq |U(t+y-D)|. \tag{168}$$

Next, by squaring the previous inequality, integrating w.r.t. y from 0 to D and passing to the square roots, we get

$$\|v(t,\cdot)\|_{L^2}^2 \leq \int_0^D |U(t+y-D)|^2 dy \tag{169}$$
$$= \int_0^D |\mathscr{F}(t+y-t_0-D, \hat{\psi}(t,\cdot,y))|^2 dy \tag{170}$$
$$= \int_0^D \left(\int_0^1 K(1,s,t+y-t_0-D)\hat{\psi}(t,s,y)\, ds\right)^2 dy \tag{171}$$
$$\leq \int_0^D \|K(1,\cdot,t+y-t_0-D)\|_{L^2(0,1)}^2 \|\hat{\psi}(t,\cdot,y)\|_{L^2(0,1)}^2 dy \tag{172}$$
$$= \int_0^D \|K(1,\cdot,t+y-t_0-D)\|_{L^2(0,1)}^2 \|\hat{z}(t+y)\|_{L^2(0,1)}^2 dy. \tag{173}$$

Seeing that $\|\hat{z}(t,\cdot)\|_{L^2(0,1)}$ is bounded for all $t \in [t_0, t_0+D+T)$ and that $\|K(1,\cdot,t-t_0-D)\|_{L^2(0,1)}$ is bounded in $[t_0, t_0+D]$, we deduce that $\|v(t,\cdot)\|_{L^2(0,D)}$ is bounded for all $t \in [t_0, t_0+D]$.

• Convergence of the control to the origin in a prescribed time:

From the expressions (146) and (153), we have for all $t \geq t_0 + D$

$$|U(t)| = |\mathscr{F}(t-t_0, \hat{\psi}(t,\cdot,D))| \tag{174}$$
$$\leq \zeta_3(t-t_0)\|z(t_0+D,\cdot)\|_{L^2(0,1)}. \tag{175}$$

In particular, it is clear that $U(t) \to 0$ when $t \to t_0+T$. This concludes the proof. ■

V. Numerical results

In this section, we present some numerical simulations for the closed-loop original system (20)-(24), the original observer system (114)-(116), as well as the original target system (127)-(131). We can either: i) implement the prescribed-time predictor-based output controller (145), with predictor variable $\hat{\varphi}(t,s,D)$ (solution to (123)-(126) at $y = D$) and observer (114)-(116) to simulate the original closed-loop system (20)-(24) first, and then via the direct transformation, to obtain the numerical solution of the target system (127)-(131). Or, ii) implement the prescribed-time predictor-based output-feedback controller $U(t)$ given in (146) with predictor variable $\hat{\psi}(t,s,D)$ (solution to (137)-(140) at $y = D$) and employing the target observer system (132)-(134). We chose the latter option, i.e., to simulate first the target systems because they are more tractable due to the "zero" at the boundary condition of the transport PDE (see (131)). Thus, using the inverse transformation, we can recover the original systems (20)-(24) and (114)-(116).

For the numerical simulations, we consider a reaction coefficient $\lambda = 11$, an initial time $t_0 = 0$, a prescribed time $T = 1$s, and 3 different delays: $D = 0.5$s, $D = 0.6$s, $D = 0.7$s. For the Parabolic PDE part (20)-(22), we consider 5 different initial conditions: $z_0(x) = 0.1(x-x^2)$, $z_0(x) = (x-x^2)$, $z_0(x) = 10(x-x^2)$, $z_0(x) = 100(x-x^2)$, and

$z_0(x) = 1000(x - x^2)$. For the transport PDE part (23)-(24) and the observer part (114)-(116), we set the initial conditions as $\hat{z}_0(x) = 0$, $v_0(y) = 0$. For the blow-up functions γ_2 and γ_3, given in (10), we take the control and observer initial gains $\gamma_{2,0} = 3.3$ and $\gamma_{3,0} = 2.2$ to satisfy the conditions (14) and (119).

We approximate the transport hyperbolic PDE parts of (20)-(24) (and (127)-(131)) using the Lax-Wendroff scheme that can be set in Shampine's solver for Matlab as presented in [16]. This solver has been useful when one wants to observe a finite-time convergence property (recall the simple transport equation with "zero" at the boundary being fixed-time convergent). The spatial and temporal discretization were done with steps $\Delta y = 2 \times 10^{-3}$, $\Delta t = 10^{-3}$ for the interval $[t_0, 0.7(t_0 + D + T))$ and $\Delta t = 5 \times 10^{-5}$ for the interval $[0.7(t_0 + D + T), t_0 + D + T)$. Notice that, in both cases, the Courant-Friedrich-Levy (CFL) condition for the numerical stability holds.

For the parabolic part of (20)-(24) (and (127)-(131)), we employ an *implicit* Euler scheme. The spatial and temporal discretization steps used were $\Delta x = 10^{-2}$, $\Delta t = 10^{-3}$ for the interval $[t_0, 0.7(t_0+D+T))$ and $\Delta t = 5\times10^{-5}$ for the interval $[0.7(t_0 + D + T), t_0 + D + T)$. This scheme is known for its unconditional stability. All integral terms involved in the infinite-dimensional direct/inverse transformations are approximated using the trapezoidal rule. Additionally, the kernel K given in (13) is explicit. It expressed in terms of exponential function and modified Bessel function of the first kind. Since it depends on time, it is recomputed at each iteration of the simulation and updating its argument, accordingly. In addition, the predictor variable $\hat{\psi}(t, s, D)$ is obtained by solving, at each iteration, (137)-(144) (still parabolic PDEs with domain $y \in [0, D]$, $x \in [0, 1]$, and fixed t) with initial condition $\hat{z}(t, x)$ begin solution to (132)-(134), and boundary conditions involving $\omega(t, y)$, solution of the transport PDE.

Figure 1 shows on the top left the evolution of $z(t, x)$, the state of reaction-diffusion PDE (20)-(22), on the top right the evolution of $\hat{z}(t, x)$, the observer state of reaction-diffusion PDE (114)-(116), on the bottom left the evolution of $v(t, y)$, the state of the transport PDE (23)-(24) and on the bottom right the evolution of $\omega(t, y)$ the state of the transport PDE (51)-(52), with the prescribed-time predictor-based output controller $U(t)$ given in (146) with $z_0(x) = 10(x-x^2)$. As it can be observed, all the states converge to the origin in a prescribed time equal to $t_0 + D + T = 1.5s$.

Figures 2 and 3 illustrate, in a logarithmic scale, two scenarios of the evolution of $J(t)$ - the norm of the closed-loop system (20)-(24), (114)-(116) with the prescribed-time predictor-based output-feedback controller $U(t)$ given in (146) in comparison with the same norm with the exponential predictor-based output-feedback controller $U_{\text{exp}}(t)$, given in (149) with the constant-gain $\lambda + \lambda_0 = 11$ involved in the control and observer kernels K_{exp} and P_{exp} given in Remark 9. In the first scenario, the initial condition is fixed as $z_0(x) = 100(x - x^2)$ and three different delays are considered: $D = 0.5$s, $D = 0.6$s, and $D = 0.7$s. In the second scenario, the delay is fixed as $D = 0.5$s and 5 different initial conditions are set: $z_0(x) = 0.1(x - x^2)$, $z_0(x) = (x - x^2)$, $z_0(x) = 10(x-x^2)$, $z_0(x) = 100(x-x^2)$, and $z_0(x) = 1000(x-x^2)$. As it can be observed, the norm of the closed-loop system (20)-(24), (114)-(116) converges to the origin in a prescribed time $t_0 + D + T$ no matter what initial condition z_0 or delay D we take.

Finally, in the upper left and right of Figure 4, we give a comparison between the norm of the closed-loop system (20)-(24), (114)-(116), for a delay $D = 0.5$s, using the prescribed-time predictor-based output-feedback controller $U(t)$ given in (146) (in red solid line) in comparison with the same norm using the exponential predictor-based controller $U_{\text{exp}}(t)$ given in (149) with the constant-gain $\lambda + \lambda_0 = 11$ (in black dashed line) and with a higher constant-gain $\lambda + \lambda_0 = 28$ (in blue dashed line). On the bottom of Figure 4, we give a comparison between the controllers $U(t)$ (in red solid line) and $U_{\text{exp}}(t)$ with the gain $\lambda + \lambda_0 = 11$ (in black dashed line) and with a higher gain $\lambda + \lambda_0 = 28$ (in blue dashed line). As it can be observed, at the delay $D = 0.5$s, the norm of the closed-loop system using the exponential controller $U_{\text{exp}}(t)$ (with the higher gain $\lambda + \lambda_0 = 28$) exhibits the "peaking phenomenon" [29] (see the blue dashed curve in the upper left plot of Figure 4). After delay $D = 0.5$s, the norm outpaces the same norm using the prescribed-time controller $U(t)$. However, as time progresses, the curves of the two norms cross, and from then on the norm of the closed-loop system using the prescribed-time controller $U(t)$ outperforms the same norm using the exponential controller $U_{\text{exp}}(t)$. This is due to the fact that the exponential controller starts with an aggressive control effort, because of the high gain $\lambda + \lambda_0$, but with time its effort diminishes (see bottom left of Figure 4). In contrast, the prescribed-time controller $U(t)$ starts with a moderate effort to avoid peeking (see [28, Section 1.4.2] for more discussions on prescribed-time controllers and their effect to reducing state peaking) and then gradually increases its control effort towards the end of the simulation to ensure that the convergence is completed in the prescribed time (see the upper left and bottom plots of Figure 4).

Remark 10: Notice that, from both theoretical and numerical point of view, there is no delay limit. In fact, one of the features of our approach is that it enables compensation for arbitrarily long delays. However, it should be noted that for very long delays D, it is necessary to reduce the space step Δy to be able to better solve the hyperbolic PDE since it is defined on delay dependent space interval $[0, D]$. In simulations, this will, of course, burden the computation effort and simulations will take longer to complete.

VI. Conclusion

This paper dealt with the problem of output-feedback stabilization in prescribed time of a 1D reaction-diffusion system with boundary input delay. The system is rewritten into a PDE-PDE setting (a cascade of a parabolic PDE with a hyperbolic PDE), where the hyperbolic PDE models the effect of the delay on the input. The predictor-based output controller is designed using a time-varying infinite-dimensional backstepping

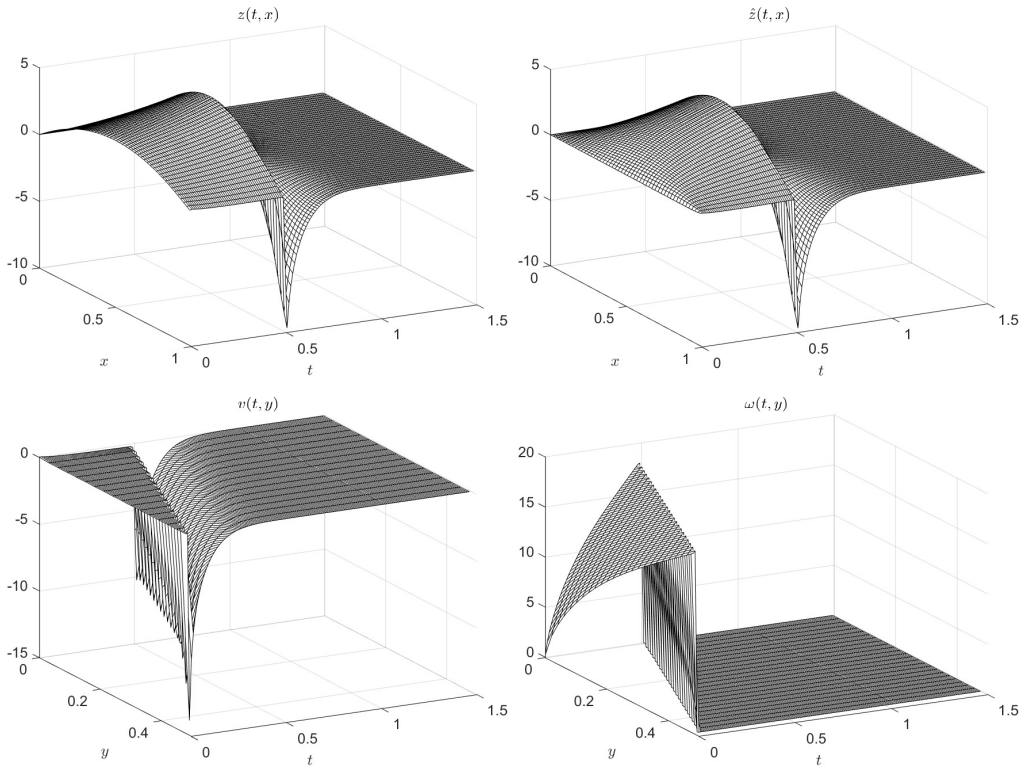

Fig. 1. On the top left: the evolution of the state $\boldsymbol{z(t,x)}$ of the parabolic PDE (20)-(22) with $\boldsymbol{z(t_0,x) = 10(x-x^2)}$. On the top right: the evolution of the observer state $\boldsymbol{\hat{z}(t,x)}$ of the parabolic PDE (114)-(116) with $\boldsymbol{\hat{z}(t_0,\cdot) \equiv 0}$. On the bottom left: the evolution of $\boldsymbol{v(t,y)}$ the state of the hyperbolic PDE (23)-(24) with prescribed-time predictor-based controller $\boldsymbol{U(t)}$ in (146) with $\boldsymbol{v(t_0,\cdot) \equiv 0}$ and $\boldsymbol{D = 0.5}$s. On the bottom right: the evolution of $\boldsymbol{\omega(t,y)}$ the state of the transport PDE (51)-(52).

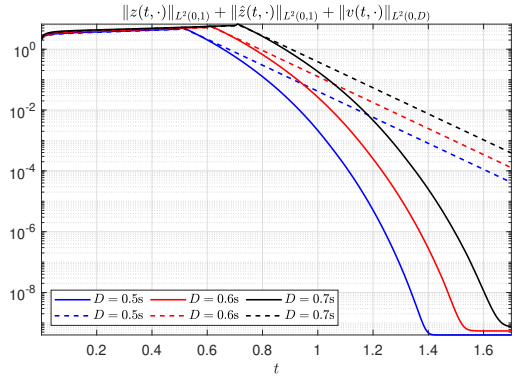

Fig. 2. The evolution of the norm $\|\boldsymbol{z(t,\cdot)}\|^2_{\boldsymbol{L^2(0,1)}} + \|\boldsymbol{\hat{z}(t,\cdot)}\|^2_{\boldsymbol{L^2(0,1)}} + \|\boldsymbol{v(t,\cdot)}\|^2_{\boldsymbol{L^2(0,D)}}$ of the closed-loop system (20)-(24), (114)-(116) with **PTS** controller $\boldsymbol{U(t)}$ (146) in solid lines and with **ES** controller $\boldsymbol{U_{\text{exp}}(t)}$ (149) with $\boldsymbol{\lambda_0 = 0}$ in dashed lines (logarithmic scale), for $\boldsymbol{z(t_0,x) = 10(x-x^2)}$, $\boldsymbol{\hat{z}(t_0,x) = 0}$, $\boldsymbol{v(t_0,y) = 0}$, and 3 different delays: $\boldsymbol{D = 0.5}$s, $\boldsymbol{D = 0.6}$s, and $\boldsymbol{D = 0.7}$s.

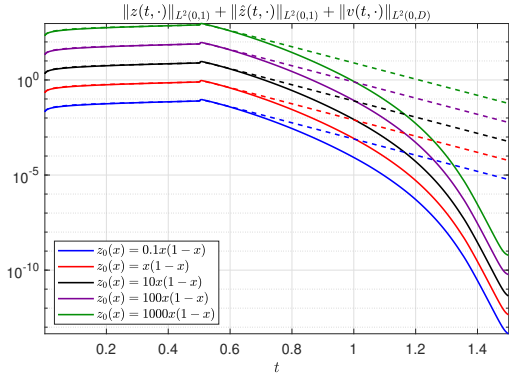

Fig. 3. The evolution of the norm $\|\boldsymbol{z(t,\cdot)}\|^2_{\boldsymbol{L^2(0,1)}} + \|\boldsymbol{\hat{z}(t,\cdot)}\|^2_{\boldsymbol{L^2(0,1)}} + \|\boldsymbol{v(t,\cdot)}\|^2_{\boldsymbol{L^2(0,D)}}$ of the closed-loop system (20)-(24), (114)-(116) with the **PTS** controller $\boldsymbol{U(t)}$ (146) in solid lines and with **ES** controller $\boldsymbol{U_{\text{exp}}(t)}$ (149) with $\boldsymbol{\lambda_0 = 0}$ in dashed lines (logarithmic scale) for a delay $\boldsymbol{D = 0.5}$ and 5 different initial conditions $\boldsymbol{z(t_0,x) = 10^i(x-x^2)}$, $\boldsymbol{i \in \{-1,0,1,2,3\}}$.

transformation that transforms the PDE-PDE unstable system into a well-chosen target system. The inverse transformation ensures the desired convergence. Numerical simulations are given to illustrate the results. Future work will extend this result to a more general class of nonlinear reaction-diffusion-advection systems with non-delayed/delayed boundary control, for which we may follow the Control Lyapunov function (CLF) technique [33]. Extensions will also include more complex dynamics, e.g., stabilization in prescribed time of parabolic PDEs coupled with hyperbolic quasilinear/semilinear equations with non-local terms for which we can also use the results in [7]. Moreover, we may consider implementation of the continuous-time controller in the light of sampled-data and event-triggered control for PDEs which requires a careful study of robustness to sampling while accounting, in this case, for time-varying growth gains and the input delay. This may

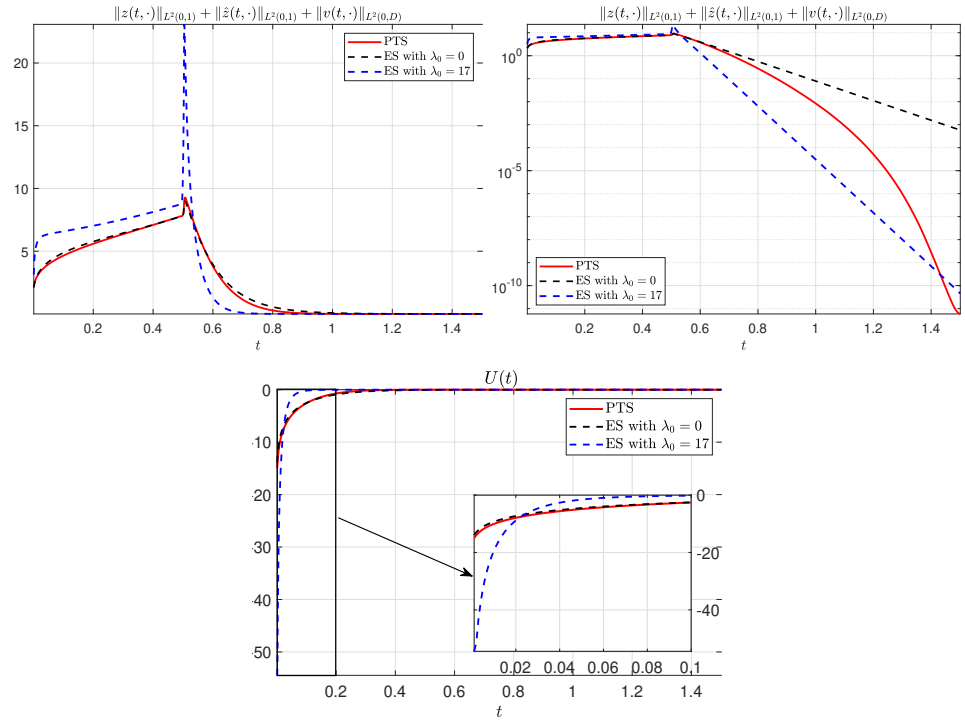

Fig. 4. On the top: The evolution of the norm $\|\boldsymbol{z(t,\cdot)}\|^{\boldsymbol{2}}_{\boldsymbol{L^2(0,1)}} + \|\boldsymbol{\hat{z}(t,\cdot)}\|^{\boldsymbol{2}}_{\boldsymbol{L^2(0,1)}} + \|\boldsymbol{v(t,\cdot)}\|^{\boldsymbol{2}}_{\boldsymbol{L^2(0,D)}}$ of the closed-loop system (20)-(24) with **PTS** controller $\boldsymbol{U(t)}$ (146) in red solid line and with **ES** controller $\boldsymbol{U_{\text{exp}}(t)}$ (149) for $\boldsymbol{\lambda_0 = 0}$ in black dashed line and $\boldsymbol{\lambda_0 = 17}$ in blue dashed line (normal scale on the left and logarithmic scale on the right), with $\boldsymbol{z(t_0,x) = 10(x - x^2)}$, $\boldsymbol{\hat{z}(t_0,x) = 0}$, $\boldsymbol{v(t_0,y) = 0}$, and $\boldsymbol{D = 0.5}$s. On the bottom, the evolution of the **PTS** controller $\boldsymbol{U(t)}$ (146) in red solid line along with **ES** controller $\boldsymbol{U_{\text{exp}}(t)}$ (149) for $\boldsymbol{\lambda_0 = 0}$ in black dashed line and $\boldsymbol{\lambda_0 = 17}$ in blue dashed line.

follow the ideas of [12].

Appendix I
Proof of Proposition 1

Let A be defined as follows:

$$A = \int_0^D \xi_2(t+y-t_0-D)^2 dy \tag{176}$$

$$:= \frac{c_l M}{(2\alpha_0)^4} \int_0^D (2\alpha_0)^4 \gamma_2(t+y-t_0-D)^2 \times e^{-2\alpha_0\sqrt{\gamma_2(t+y-t_0-D)}} dy \tag{177}$$

$$= \frac{c_l M}{(2\alpha_0)^4} \int_0^D (2\alpha_0\sqrt{\gamma_2(t+y-t_0-D)})^4 \times e^{-2\alpha_0\sqrt{\gamma_2(t+y-t_0-D)}} dy. \tag{178}$$

where M, c_k, and α_0 are all defined in (16).

Next, let us consider the following change of variables:

$$s = 2\alpha_0\sqrt{\gamma_2(t+y-t_0-D)} = \frac{2\alpha_0\gamma_{2,0}T}{(t_0+D+T-t-y)} \tag{179}$$

from which we recover,

$$\frac{ds}{dy} = \frac{2\alpha_0\gamma_{2,0}T}{(t_0+D+T-t-y)^2} = \frac{2\alpha_0}{\gamma_{2,0}T}\gamma_2(t+y-t_0-D) = \frac{s^2}{2\alpha_0\gamma_{2,0}T}. \tag{180}$$

Now, by using (179)-(180) in (176) (along with $dy = 2\alpha_0\gamma_{2,0}T\frac{ds}{s^2}$), we obtain

$$A = \frac{\gamma_{2,0}c_l MT}{8\alpha_0^3} \int_{2\alpha_0\sqrt{\gamma_2(t-t_0-D)}}^{2\alpha_0\sqrt{\gamma_2(t-t_0)}} s^2 e^{-s} ds \tag{181}$$

Finally, by integrating by parts twice, we recover

$$\begin{aligned} A &= \frac{\gamma_{2,0}c_l MT}{8\alpha_0^3} \left[-(s^2+2s+2)e^{-s}\right]_{2\alpha_0\sqrt{\gamma_2(t-t_0-D)}}^{2\alpha_0\sqrt{\gamma_2(t-t_0)}} \\ &= -Q\Big(2\alpha_0\sqrt{\gamma_2(t-t_0)}\Big)e^{-2\alpha_0\sqrt{\gamma_2(t-t_0)}} \\ &\quad + Q\Big(2\alpha_0\sqrt{\gamma_2(t-t_0-D)}\Big)e^{-2\alpha_0\sqrt{\gamma_2(t-t_0-D)}} \\ &\leq Q\Big(2\alpha_0\sqrt{\gamma_2(t-t_0-D)}\Big)e^{-2\alpha_0\sqrt{\gamma_2(t-t_0-D)}}, \end{aligned} \tag{182}$$

where $Q(s) = \frac{\gamma_{2,0}c_l MT}{8\alpha_0^3}(s^2+2s+2)$.
This concludes the proof.

Appendix II
Proof of Proposition 3

Let B be defined as follows,

$$B = \int_0^D \zeta_3(t+y-t_0-D)^2 dy := \int_0^D Q_3\big(\alpha_3\gamma_1(t+y-t_0-D)\big) \times e^{-\alpha_3\gamma_1(t+y-t_0-D)} dy, \tag{183}$$

where ζ_3 is given in (111).

Next, let us consider the following change of variables:

$$\begin{aligned} s &= \alpha_3\gamma_1(t+y-t_0-D) \\ &= \frac{\alpha_3\gamma_{1,0}T}{(t_0+D+T-t-y)}, \end{aligned} \tag{184}$$

from which we recover,

$$\begin{aligned} \frac{ds}{dy} &= \frac{\alpha_3\gamma_{1,0}T}{(t_0+D+T-t-y)^2} \\ &= \frac{\alpha_3}{\gamma_{1,0}T}\gamma_2(t+y-t_0-D) \\ &= \frac{s^2}{\alpha_3\gamma_{1,0}T}. \end{aligned} \tag{185}$$

Now, by using (184)-(185) in (183) (along with $dy = \alpha_3\gamma_{1,0}T\frac{ds}{s^2}$), we obtain

$$B = \alpha_3\gamma_{1,0}T\int_{\alpha_3\gamma_1(t-t_0-D)}^{\alpha_3\gamma_1(t-t_0)} \frac{Q_3(s)}{s^2}e^{-s}ds. \tag{186}$$

By noticing that the polynomial function $Q_3(\cdot)$ (of degree $p \in \mathbb{N}^*$) can be expressed as $Q_3(s) = \sum_{i=0}^{p} c_i s^i$ with some positive coefficients $c_i > 0$, we get,

$$B = \alpha_3\gamma_{1,0}T\sum_{i=0}^{p} c_i \int_{\alpha_3\gamma_1(t-t_0-D)}^{\alpha_3\gamma_1(t-t_0)} s^{i-2}e^{-s}ds. \tag{187}$$

Now, let us calculate each sub-integral of the previous expression. To do that, let us consider the following two cases:

Case 1: Let $i \in \{2,3,\cdots,p\}$ (i.e. $i-2 \geq 0$). Then, by using multiple integrations by parts, we obtain,

$$\int_{\alpha_3\gamma_1(t-t_0-D)}^{\alpha_3\gamma_1(t-t_0)} s^{i-2}e^{-s}ds = \left[-(i-2)!\sum_{j=0}^{i-2}\frac{s^j}{j!}e^{-s}\right]_{\alpha_3\gamma_1(t-t_0-D)}^{\alpha_3\gamma_1(t-t_0)} \tag{188}$$

$$\leq (i-2)!\sum_{j=0}^{i-2}\frac{(\alpha_3\gamma_1(t-t_0-D))^j}{j!}e^{-\alpha_3\gamma_1(t-t_0-D)}. \tag{189}$$

Note that proving (188) is straightforward by induction.

Case 2: Let $i \in \{0,1\}$ (i.e. $i-2 < 0$). Then, by using the generalized exponential, defined as

$$E_n(r) = r^{n-1}\int_r^{\infty}\frac{e^{-s}}{s^n}ds, \quad r>0, n\in\mathbb{N}^*, \tag{190}$$

and its property [3, Section 2]:

$$\frac{e^{-r}}{n+r} \leq E_n(r) \leq \frac{e^{-r}}{n-1+r}, \tag{191}$$

we obtain,

$$\int_{\alpha_3\gamma_1(t-t_0-D)}^{\alpha_3\gamma_1(t-t_0)}\frac{e^{-s}}{s^{2-i}}ds \leq \int_{\alpha_3\gamma_1(t-t_0-D)}^{+\infty}\frac{e^{-s}}{s^{2-i}}ds \tag{192}$$

$$:= \frac{1}{(\alpha_3\gamma_1(t-t_0-D))^{1-i}}E_{2-i}(\alpha_3\gamma_1(t-t_0-D)) \tag{193}$$

$$\leq \frac{e^{-\alpha_3\gamma_1(t-t_0-D)}}{(1-i+\alpha_3\gamma_1(t-t_0-D))(\alpha_3\gamma_1(t-t_0-D))^{1-i}}. \tag{194}$$

Finally, by using (189) from Case 1 and (194) from Case 2, we recover,

$$B \leq Q_4(\alpha_3\gamma_1(t-t_0-D))e^{-\alpha_3\gamma_1(t-t_0-D)}, \tag{195}$$

where

$$\begin{aligned} Q_4(s) = \alpha_3\gamma_{1,0}T\Bigg(&\sum_{i=0}^{1}\frac{c_i}{(1-i+s)s^{1-i}} \\ &+\sum_{i=2}^{p}c_i(i-2)!\sum_{j=0}^{i-2}\frac{s^j}{j!}\Bigg). \end{aligned} \tag{196}$$

This concludes the proof.

ACKNOWLEDGMENT

We would like to thank Drew Steeves for the fruitful discussions on prescribed-time control for PDEs.

REFERENCES

[1] S. Bhat and D. Bernstein. Lyapunov analysis of finite-time differential equations. In *Proceedings of 1995 American Control Conference*, volume 3, pages 1831–1832. IEEE, 1995.

[2] S. Chen, M. Krstic, and R. Vazquez. Backstepping boundary control of a 1-D 2 × 2 unstable diffusion-reaction PDE system with distinct input delays. In *2019 American Control Conference (ACC)*, pages 2564–2569, 2019.

[3] C. Chiccoli, S. Lorenzutta, and G. Maino. Recent results for generalized exponential integrals. *Computers & Mathematics with Applications*, 19:21–29, Dec. 1990.

[4] J. Deutscher and J. Gabriel. Fredholm backstepping control of coupled linear parabolic PDEs with input and output delays. *IEEE Transactions on Automatic Control*, 65(7):3128–3135, 2020.

[5] I. A. Djebour, T. Takahashi, and J. Valein. Feedback stabilization of parabolic systems with input delay. *Mathematical Control and Related Fields*, 12(2):405–420, 2022.

[6] N. Espitia, A. Polyakov, D. Efimov, and W. Perruquetti. Boundary time-varying feedbacks for fixed-time stabilization of constant-parameter reaction-diffusion systems. *Automatica*, 103, 2019.

[7] A. Irscheid, N. Espitia, W. Perruquetti, and J. Rudolph. Prescribed-time control for a class of semilinear hyperbolic PDE-ODE systems. *IFAC-PapersOnLine*, 55(26):47–52, 2022. 4th IFAC Workshop on Control of Systems Governed by Partial Differential Equations CPDE 2022.

[8] I. Karafyllis. Finite-time global stabilization by means of time-varying distributed delay feedback. *SIAM J. Control Optim.*, 45:320–342, 2006.

[9] R. Katz and E. Fridman. Delayed finite-dimensional observer-based control of 1-D parabolic PDEs. *Automatica*, 123:109364, 2021.

[10] R. Katz, E. Fridman, and A. Selivanov. Boundary delayed observer-controller design for reaction–diffusion systems. *IEEE Transactions on Automatic Control*, 66(1):275–282, 2021.

[11] S. Koga, D. Bresch-Pietri, and M. Krstic. Delay compensated control of the stefan problem and robustness to delay mismatch. *International Journal of Robust and Nonlinear Control*, 30(6):2304–2334, 2020.

[12] F. Koudohode, N. Espitia, and M. Krstic. Event-triggered boundary control of an unstable reaction diffusion pde with input delay. *To appear in Systems and Control Letters*, 2024.

[13] M. Krstic. Control of an unstable reaction-diffusion PDE with long input delay. *Systems & Control Letters*, 58:773–782, Dec. 2009.

[14] M. Krstic. *Delay Compensation for Nonlinear, Adaptive, and PDE Systems*. Birkhäuser Basel, Jan. 2009.

[15] M. Krstic and A. Smyshlyaev. *Boundary Control of PDEs: A Course on Backstepping Designs*. Society for Industrial and Applied Mathematics, Jan. 2008.

[16] L.F. Shampine. Solving hyperbolic PDEs in MATLAB. *Applied Numerical Analysis & Computational Mathematics*, 2(3):346–358, 2005.

[17] W. Michiels and B. Zhou. On the fixed-time stabilization of input delay systems using act-and-wait control. *Systems & Control Letters*, 146, 2020.

[18] E. Moulay, M. Dambrine, N. Yeganefar, and W. Perruquetti. Finite-time stability and stabilization of time-delay systems. *Systems & Control Letters*, 57:561–566, 2008.

[19] N. Espitia and W. Perruquetti. Predictor-feedback Prescribed-time stabilization of LTI systems with input delay. *IEEE Transactions on Automatic Control*, 67(6), 2021.
[20] A. Polyakov. Nonlinear feedback design for fixed-time stabilization of linear control systems. *IEEE Transactions on Automatic Control*, 57(8):2106–2110, 2012.
[21] A. Polyanin and V. Nazaikinskii. *Handbook of Linear Partial Differential Equations for Engineers and Scientists, Second Edition*. CRC Press, 01 2016.
[22] C. Prieur and E. Trélat. Feedback stabilization of a 1-D linear reaction–diffusion equation with delay boundary control. *IEEE Transactions on Automatic Control*, 64(4):1415–1425, 2019.
[23] J. Qi and M. Krstic. Compensation of spatially varying input delay in distributed control of reaction-diffusion PDEs. *IEEE Transactions on Automatic Control*, 66(9):4069–4083, 2021.
[24] H. Sano. Neumann boundary stabilization of one-dimensional linear parabolic systems with input delay. *IEEE Transactions on Automatic Control*, 63(9):3105–3111, 2018.
[25] Y. Song, Y. Wang, J. Holloway, and M. Krstic. Time-varying feedback for regulation of normal-form nonlinear systems in prescribed finite time. *Automatica*, 83:243–251, 09 2017.
[26] D. Steeves, N. Espitia, M. Krstic, and W. Perruquetti. Input delay compensation in prescribed-time of boundary-actuated reaction-diffusion PDEs. In *2021 American Control Conference (ACC)*, pages 274–279, May 2021.
[27] D. Steeves, M. Krstic, and R. Vazquez. Prescribed-time stabilization of reaction-diffusion equation by output feedback. In *2019 American Control Conference (ACC)*, pages 2570–2575, 2019.
[28] D. A. Steeves. *Prescribed-Time and Safety-Critical Control for Nonlinear and Distributed-Parameter Systems*. Theses, UC San Diego Electronic Theses and Dissertations, 2022.
[29] H. Sussmann and P. Kokotovic. The peaking phenomenon and the global stabilization of nonlinear systems. *IEEE Transactions on Automatic Control*, 36(4):424–440, 1991.
[30] S. Wang, J. Qi, and M. Diagne. Adaptive boundary control of reaction–diffusion PDEs with unknown input delay. *Automatica*, 134:109909, 2021.
[31] S. Zekraoui, N. Espitia, and W. Perruquetti. Prescribed-time predictor control of LTI systems with distributed input delay. In *60th IEEE Conference on Decision and Control (CDC)*, pages 1850–1855, Dec. 2021.
[32] S. Zekraoui, N. Espitia, and W. Perruquetti. Finite, fixed-time stabilization of a chain of integrators with input delay via PDE-based nonlinear backstepping approach. *Automatica*, 2023.
[33] S. Zekraoui, N. Espitia, and W. Perruquetti. Lyapunov-based nonlinear boundary control design with predefined convergence for a class of 1d linear reaction-diffusion equation. *European Journal of Control*, 74, 2023. 2023 European Control Conference Special Issue.
[34] Z. Zuo. Fixed-time stabilization of general linear systems with input delay. *Journal of the Franklin Institute*, 356(8):4467–4477, 2019.

Salim Zekraoui holds a Bachelor of Science degree in Mathematics and a Master of Science degree in Applied Mathematics focused on numerical analysis of partial differential equations, from École Normale Supérieure (ENS) in Casablanca. In November 2023, he completed his Ph.D. degree at Centrale Lille institute. Since January 2024, he has been a Postdoctoral Researcher with LAGEPP - Univ. Lyon 1. His research interests center around stabilization and estimation of PDEs and time delay systems.

Nicolás Espitia received the B.S. degree in electronic engineering and the second B.S. degree in mathematics from the Escuela Colombiana de Ingeniería Julio Garavito, Bogota, Colombia, in 2011 and 2012, respectively, the M.S. degree in systems, control, and information technology from Université Joseph Fourier, Grenoble, France, in 2014, and the Ph.D. degree in control systems from the GIPSA-Lab, Grenoble University, Grenoble, in 2017. From 2017 to 2019, he was a Postdoctoral Researcher with Inria Lille Nord-Europe. Since October 2019, he has been a CNRS Researcher with the Centre de Recherche en Informatique, Signal et Automatique de Lille, Lille, France. His research interests include event-triggered boundary control and finite-/fixed-/prescribed-time stabilization and estimation of partial differential equations.

Wilfrid Perruquetti received his graduate degree in automatic control from the Institut Industriel du Nord (now Centrale Lille Institut), Lille, France, in 1991, and his Ph.D. degree in automatic control from "École Centrale de Lille" in 1994. In 1995, he joined Centrale Lille Institut as an Assistant Professor, where he is currently a Full Professor. His research interests include stability analysis (encompassing various stability concepts), finite-time stabilization, sliding-mode control of nonlinear and delay systems, state observation, and system parameter identification. Dr. Perruquetti served as Vice-Deputy of the Institute for Information Sciences and Technologies, CNRS, from 2014 to 2017, as a Project Manager with the French National Research Agency from 2010 to 2014, and as a Representative of the French Ministry of Education and Research from 2007 to 2009.

Miroslav Krstic is Distinguished Professor and Senior Associate Vice Chancellor for Research at UC San Diego. Krstic is Fellow of IEEE, IFAC, ASME, SIAM, AAAS, IET (UK), and AIAA (Assoc. Fellow) - and member of the Serbian Academy of Sciences. He has received the Bode Lecture Prize, Bellman Award, SIAM Reid Prize, ASME Oldenburger Medal, Nyquist Lecture Prize, Paynter Outstanding Investigator Award, Ragazzini Education Award, IFAC Nonlinear Control Systems Award, IFAC Distributed Parameter Systems Award, IFAC Adaptive and Learning Systems Award, Chestnut textbook prize, Control Systems Society Distinguished Member Award, the PECASE, NSF Career, and ONR Young Investigator awards, the Schuck (96 and 19) and Axelby paper prizes. He serves as Editor-in-Chief of Systems & Control Letters and has been serving as Senior Editor in Automatica and IEEE Transactions on Automatic Control.